

TKK Dissertations 48
Espoo 2006

**MODELLING AND EXPERIMENTAL STUDY ON WOOD
CHIPS BOILER SYSTEM WITH FUEL DRYING AND
WITH DIFFERENT HEAT EXCHANGERS**

Doctoral Dissertation

Jukka Yrjölä



**Helsinki University of Technology
Department of Mechanical Engineering
Laboratory of Applied Thermodynamics**

TKK Dissertations 48
Espoo 2006

**MODELLING AND EXPERIMENTAL STUDY ON WOOD
CHIPS BOILER SYSTEM WITH FUEL DRYING AND
WITH DIFFERENT HEAT EXCHANGERS**

Doctoral Dissertation

Jukka Yrjölä

Dissertation for the degree of Doctor of Science in Technology to be presented with due permission of the Department of Mechanical Engineering for public examination and debate in Micronova at Helsinki University of Technology (Espoo, Finland) on the 16th of November, 2006, at 12 noon.

**Helsinki University of Technology
Department of Mechanical Engineering
Laboratory of Applied Thermodynamics**

**Teknillinen korkeakoulu
Konetekniikan osasto
Sovelletun termodynamiikan laboratorio**

Distribution:

Helsinki University of Technology
Department of Mechanical Engineering
Laboratory of Applied Thermodynamics
P.O. Box 4400
FI - 02015 TKK
FINLAND
URL: <http://www.termo.hut.fi/>
Tel. +358-9-451 3581
Fax. +358-9-455 3724
E-mail: terhi.kujala@tkk.fi

© 2006 Jukka Yrjölä

ISBN-13 978-951-22-8438-2
ISBN-10 951-22-8438-3
ISBN-13 978-951-22-8439-9 (PDF)
ISBN-10 951-22-8439-1 (PDF)
ISSN 1795-2239
ISSN 1795-4584 (PDF)
URL: <http://lib.tkk.fi/Diss/2006/isbn9512284391/>

TKK-DISS-2199

Edita Oy
Helsinki 2006



HELSINKI UNIVERSITY OF TECHNOLOGY P. O. BOX 1000, FI-02015 TKK http://www.tkk.fi		ABSTRACT OF DOCTORAL DISSERTATION	
Author Jukka Yrjölä			
Name of the dissertation Modelling and Experimental Study on Wood Chips Boiler System with Fuel Drying and with Different Heat Exchangers			
Date of manuscript 08.06.2006		Date of the dissertation 16.11.2006	
<input type="checkbox"/> Monograph		<input checked="" type="checkbox"/> Article dissertation (summary + original articles)	
Department	Mechanical Engineering		
Laboratory	Applied Thermodynamics		
Field of research	Applied Thermodynamics		
Opponent(s)	Professor Esa Marttila, Professor Roland Wimmerstedt		
Supervisor (Instructor)	Professor Markku Lampinen Dr. Jaakko Saastamoinen		
Abstract <p>This thesis introduces two types of boiler plants with a cross-flow warm air moving bed dryer. The first one dries wood chips for the use of the plant itself. The second one is also equipped with a sieve and it even produces fuel to the market, to the small-scale boilers, for example. This has notable technical benefits because the load of the boiler plant is more stable than that in the traditional district heating use. Good quality wood fuel also improves the operation and control of small-scale heating systems of customers, which can lead to cheaper furnaces with lower emissions.</p> <p>There are interdependencies between the dryer, boiler and heat exchangers, which are the main equipments under study. In addition, the ranges of heating load, of moisture content of fuel and of outdoors air temperature are large. Therefore, models were developed for improved understanding and prediction of the thermal performance of the system and for technical optimisation of equipment. Six models are described, two for each equipment under study.</p> <p>Energy and mass balance model and a deep bed model for drying were developed. The deep bed model bases on the shrinking core single-particle model. A model was developed to calculate the heat transfer rate and pressure loss of the convection section with tubes and another one for the convection section with a rectangular duct having an array of longitudinal rectangular fins for flue gas. Two heat exchangers are described and modelled, a pipe-bundle type flue gas heat exchanger and a flat plate type heat exchanger, which recovers heat from the drying exhaust gas. Case analyses for energy consumption and equipment dimensioning are described.</p> <p>The models for a dryer were verified by the measurements on the laboratory test rig and other models on the 40 kW_{th} pilot plant and on the 500 kW_{th} demonstration plant and on three other boiler plants. Only the results of the model for convection section indicated an excessive difference between the measurements. All other models gave results in reasonably close accordance with the measurements.</p>			
Keywords	bed, bioenergy, chip, fin, fouling, heat transfer, wood chip		
ISBN (printed)	951-22-8438-3	ISSN (printed)	1795-2239
ISBN (pdf)	951-22-8439-1	ISSN (pdf)	1795-4584
ISBN (others)		Number of pages	65 p.+97 app.
Publisher	Helsinki University of Technology, Dept. of Mechanical Eng., Lab. of Applied Thermodynamics		
Print distribution	Helsinki University of Technology, Dept. of Mechanical Eng., Lab. of Applied Thermodynamics		
<input checked="" type="checkbox"/> The dissertation can be read at http://lib.tkk.fi/Diss/2006/isbn9512284391			



TEKNILLINEN KORKEAKOULU PL 1000, 02015 TKK http://www.tkk.fi		VÄITÖSKIRJAN TIIVISTELMÄ	
Tekijä Jukka Yrjölä			
Väitöskirjan nimi Polttoainekuivauksen ja lämmönsiirtimiä sisältävän hakekattilalaitoksen mallinnus ja mittaukset			
Käsikirjoituksen jättämispäivämäärä 08.06.2006		Väitöstilaisuuden ajankohta 16.11.2006	
<input type="checkbox"/> Monografia		<input checked="" type="checkbox"/> Yhdistelmäväitöskirja (yhteenvedo + erillisartikkelit)	
Osasto	Konetekniikka		
Laboratorio	Sovellettu termodynamiikka		
Tutkimusala	Sovellettu termodynamiikka		
Vastaväittäjät	Professori Esa Marttila, professori Rolan Wimmerstedt		
Työn valvoja	Professori Markku Lampinen		
Työn ohjaaja	TKT Jaakko Saastamoinen		
Tiivistelmä			
<p>Tässä väitöskirjassa kuvataan kahta hakekattilalaitosta, joissa haketta kuivataan ristivirtatyypisellä jatkuvatoimisella lämminilmakuivurilla. Toinen kuivaa haketta laitoksen omaan käyttöön ja toinen seulalla varustettuna kuivaa sitä myös myyntiin esimerkiksi pienille kattiloille. Kuivatun ja seulotun hakkeen tuotanto tasaa kattilan kuormitusta, mikä on edullista sen toiminnalle. Tuotettu laadukas hake tehostaa myös pienten loppukäyttäjäkattiloiden toimintaa ja helpottaa niiden säätöä, mikä voi pienentää päästöjä ja johtaa halvempiin laitoksiin.</p> <p>Väitöskirja keskittyy laitoksen polttoainekuivuriin, kattilaan ja lämmönsiirtimiin. Ne ovat keskenään vuorovaikutuksessa ja lisäksi lämmitystehontarpeen, polttoaineen kosteuden ja ulkoilman lämpötilan vaihtelut ovat suuria. Siksi työssä kehitettiin laskentamalleja, jotka helpottavat laitoskokonaisuuden toiminnan ymmärtämistä ja suorituskyvyn ennakoimista sekä yksittäisten laitteiden optimointia. Työssä kuvataan kuutta laskentamallia, joista kuhunkin kolmeen päälaitteeseen liittyy kaksi mallia.</p> <p>Kuivurille laadittiin yksinkertainen energia- ja massatasemalli. Lisäksi kehitettiin paksun hakekerroksen kuivumista kuvaava malli, joka ottaa huomioon myös massan siirtymisen hakepartikkelin sisällä. Kattilan konvektio-osan kaksi eri rakennetta mallinnettiin. Toinen malli kuvaa pyöreäputkista konvektio-osaa ja toisessa savukaasukanava on poikkipinnaltaan suorakaiteenmuotoinen, ja siinä on pitkittäiset tasapaksut levyrivat. Lisäksi mallinnettiin kattilan savukaasusta kuivausilmaan lämpöä siirtävä putkinippulämmönsiirrin ja kuivurin poistokaasusta kuivausilmaan lämpöä siirtävä levylämmönsiirrin. Energiankulutusta ja laitemitoitusta havainnollistetaan esimerkein.</p> <p>Kuivurimallia verifioitiin laboratoriomittauksin ja muita malleja mittauksin 40 kW_{th} pilottilaitoksessa ja 500 kW_{th} demonstraatiolaitoksessa sekä kolmessa muussa kattilalaitoksessa. Mallit antoivat kohtuullisen hyvin mittauksien kanssa yhtäpitäviä tuloksia, ainoastaan konvektio-osan malli poikkesi paljon.</p>			
Asiasanat bioenergia, hake, kuivaus, likaantuminen, lämmönsiirto, ripa			
ISBN (painettu)	951-22-8438-3	ISSN (painettu)	1795-2239
ISBN (pdf)	951-22-8439-1	ISSN (pdf)	1795-4584
ISBN (muut)		Sivumäärä	65 s. + 97 s. liitteitä
Julkaisija TKK Konetekniikan osasto Sovelletun termodynamiikan laboratorio			
Painetun väitöskirjan jakelu TKK Konetekniikan osasto Sovelletun termodynamiikan laboratorio			
<input checked="" type="checkbox"/> Luettavissa verkossa osoitteessa http://lib.tkk.fi/Diss/2006/isbn9512284391			

PREFACE

First I would like to thank my supervising Professor Markku Lampinen for his patience in advising me during this work. He has been my idol in the field of thermal science ever since he was the supervisor of my graduate thesis. I am especially indebted to my instructor Dr. Jaakko Saastamoinen. His insight and enthusiasm in the science of mathematical modelling has inspired me decisively. His reliability and always prompt, rigorous and useful comments have been indispensable. I would like to thank my pre-examiners Professor Arun S. Mujumdar and Professor Esa Marttila for their suggestions.

This study was carried out during the years 1998 through 2006 in the Satakunta University of Applied Sciences. I would like to thank Dr. Matti Lähdeniemi for encouragement and for providing me the opportunity to accomplish this thesis work. I thank Mr. Martti Honkasalo for many inspiring discussions. He is the inventor of the first modelled drying system. I am especially indebted to Mr. Janne Paavilainen for his skills and diligence in spreadsheet computation and field experiments. We have sat countless evenings together at the computer trying to make models work and to eliminate the bugs. The colleagues deserve thanks for smooth co-operation. I express my gratitude towards all of my co-authors and other people who have been involved in the study. The financial support of Tekes (the Finnish Funding Agency for Technology and Innovation), Nakkila Works, Thermia Inc. and the High Technology Foundation in Satakunta is gratefully acknowledged.

Finally, I wish to thank my wife, Leena, for her patience and support. Leena and my both sons have unselfishly given up much to allow me to do this study.

Modelling and Experimental Study on Wood Chips Boiler System with Fuel Drying and with Different Heat Exchangers

CONTENTS

ABSTRACT

PREFACE

CONTENTS

LIST OF PAPERS

AUTHOR'S CONTRIBUTION

LIST OF SYMBOLS AND ABBREVIATIONS

1. INTRODUCTION	11
2. BIOMASS BOILER PLANT	18
2.1 Design aspects of the boiler plant	18
2.2 Biomass boiler plant with dryer and heat exchangers	20
2.2.1 Drying of fuel for the own use	20
2.2.2 Drying of fuel for market	21
2.3 Discussion	23
3. DRYER	25
3.1 Modelling	25
3.1.1 Energy and mass balance model	25
3.1.2 Modelling of the deep bed	26
3.2 Analyses	28
3.2.1 Energy and mass balance	28
3.2.2 Deep bed	30

3.3 Discussion	30
4. CONVECTION SECTION OF THE BOILER	33
4.1 Convection section with tubes	33
4.1.1 Modelling	33
4.1.2 Experiment	35
4.1.3 Analyses	37
4.2 Rectangular convection section with fins	40
4.2.1 Modelling	40
4.2.2 Analyses	43
4.3 Discussion	45
5. HEAT EXCHANGER	49
5.1 Flue gas heat exchanger	49
5.1.1 Modelling	49
5.1.2 Analyses	49
5.2 Drying exhaust gas heat exchanger	53
5.2.1 Modelling	53
5.2.2 Analyses	53
5.3 Discussion	56
6. CONCLUSIONS	58

REFERENCES

APPENDICES A - F (Papers I – VI)

LIST OF PAPERS

This thesis consists of a review of the following six studies which are subsequently denoted as Papers I – VI and shown in Appendices A - F:

- I Yrjölä J. Model and simulation of heat exchangers and drying silo in a new type of a boiler plant. Conference on Progress in Thermochemical Biomass Conversion. Tyrol, Austria, 2000. Bridgwater A.V (ed.); Blackwell Science Ltd, Cornwall, Great Britain 2001:678 - 92
- II Yrjölä J, Saastamoinen JJ. Modelling and practical operation results of a dryer for wood chips. *Drying Technology*, 2002;20 (5):1073 - 95
- III Yrjölä J, Paavilainen J. Modelling and analyses of heat exchangers in a biomass boiler plant. *Int. Journal of Energy Research* 2004;28 (6):473 - 94.
- IV Yrjölä J. Production of dry wood chips in connection with a district heating plant. *Thermal Science* 2004;8 (2):143 - 55
- V Yrjölä J, Paavilainen J, Oravainen H. Modelling of the finned convection section of a biomass boiler. *Energy Conversion and Management* 2006;47 (15 - 16):2552 - 2563
- VI Yrjölä J, Paavilainen J, Sillanpää M. Modelling and experimental studies on heat transfer in the convection section of a biomass boiler. *Int. J. Energy Research*, 2006;30 (12):939 - 953

AUTHOR'S CONTRIBUTION

Paper I introduces a boiler plant with a dryer and models for the dryer and heat exchangers. The inventor of the boiler plant system is Martti Honkasalo. The author did the mathematical modelling for energy and mass balance of dryer and for heat exchangers. Janne Paavilainen carried out the spreadsheet program and computation with the author. The author wrote the paper. Dr. Jaakko Saastamoinen (later instructor) discussed the manuscript and suggested many improvements on it.

The author did the mathematical modelling for the deep bed convective dryer in Paper II. An essential part of the model is the single-particle model, which was earlier developed by Dr. Saastamoinen and is improved in this paper by him. Janne Paavilainen carried out the spreadsheet program and computation with the author. Pekka Anttonen and Jukka Karppinen installed the test rig and Jukka Karppinen carried out the measurements. Dr. Saastamoinen wrote the chapter titled Model for Single Particle Drying and the author composed other chapters and established the comparison of sorption heat in the Appendix. The instructor discussed the manuscript and suggested many improvements on it.

Paper III discusses the flue gas heat exchanger and drying exhaust gas heat exchanger for which the author did the mathematical modelling. Aimo Hakala and Risto Soini installed the pilot plant with the mechanics at Nakkila Works. With the group of students and the author they also carried out the measurements on the pilot plant. Janne Paavilainen carried out the spreadsheet program and computation with the author and modelled the combined heat exchanger. Together with the author, Dr. Jukka-Pekka Spets, Dr. Pekka Ahtila and Tuula Vanha-aho designed the measurement program for emission measurements of the dryer in the demonstration plant. Kirsi Koivisto and the measurement group of Outokumpu Research Centre carried out the measurements. Juha Peltola, Janne Paavilainen, the author and a group of students carried out the thermal measurements on the boiler, heat exchangers and the dryer in the demonstration plant. The author wrote the paper. The co-author discussed the manuscript and edited it.

Paper IV introduces the boiler plant with a dryer which produces chips to the market in connection with district heating. The author is the inventor of the concept. Together with the author, Peter Pyykkönen carried out a spreadsheet program and computations concerning mass balances of the system. The author did the other computations and wrote the paper. The instructor discussed the manuscript and edited it.

The author did the mathematical modelling of heat transfer on the fouled fin in Paper V. Janne Paavilainen carried out the spreadsheet program and computation with the author. Jouni Vaitilo carried out the FEM-modelling and Janne Paavilainen made the computations. Janne Paavilainen, Jarmo Lundgren and the author carried out the verification measurements on the 1000 kW_{th} boiler and Heikki Oravainen conducted the laboratory measurements on the 300 kW_{th} boiler. The author wrote the paper. The co-authors and instructor discussed the manuscript and suggested improvements on it.

As for Paper VI, the author did the mathematical modelling of the entrance region of the tube. Janne Paavilainen carried out the spreadsheet program and computation with the author and conducted the verification measurements on the 4000 kW_{th} boiler. Matti Sillanpää organized verification measurements on the 50 kW_{th} pellet boiler. The author wrote the paper. The co-authors and the instructor discussed the manuscript and edited it. The manuscript was thoroughly improved by the supervisor, Professor Markku Lampinen.

LIST OF SYMBOLS AND ABBREVIATIONS

Symbols

a	distance between adjacent fins, m
A	area, m ²
c, c_p	specific heat capacity, J kg ⁻¹ K ⁻¹
C	constant
\dot{C}	heat capacity flow of the ventilation and infiltration, WK ⁻¹
d	diameter, m
D	diffusivity, m ² s ⁻¹
h	heat transfer coefficient, Wm ⁻² K ⁻¹ , specific enthalpy, Jkg ⁻¹ , height, m
h_c	heat transfer coefficient, W m ⁻² K ⁻¹
I	depth, m
k	heat conductivity, WK ⁻¹ m ⁻¹
l	heat of phase change, J kg ⁻¹ , length, m
n	number
\dot{m}	mass flow, kgs ⁻¹
\dot{m}''	mass flux, kg m ⁻² s ⁻¹
Nu	Nusselt number
P	circumference, m
R	heat transfer resistance of fouling, KmW ⁻¹ , radius, m
s	distance, m, thickness, m
S''	surface area of particles (for heat and mass transfer), m ²
S'''	surface area of particles/volume = (1 + Γ)(1 - ε)/ R , m ⁻¹
T	temperature, K
t	temperature, °C
U	wetted perimeter of flue gas, m, overall heat transfer coefficient, WK ⁻¹
u	moisture (dry basis in excess to equilibrium moisture level)
v	velocity, m s ⁻¹
x	absolute humidity, kg _{water vapour} /kg _{dry air} ⁻¹
x_d	dimensionless length
Y	mass fraction of water vapour, kg _{water vapour} /kg _{moist air} ⁻¹
z	distance between baffles, m, dimensionless length = l/d_i
q	mass flow rate, kg s ⁻¹
α	heat transfer coefficient, W m ⁻² K ⁻¹
ε	porosity
θ	temperature difference, K
λ	heat conductivity, W m ⁻¹ K ⁻¹
Φ	heat transfer rate, Wm ⁻¹
Γ	shape factor, 0 for plates, 1 for cylinders, 2 for spheres
ϕ	relative humidity
ω	moisture content, wet basis

Subscripts

<i>a</i>	air
<i>b</i>	base
<i>c</i>	convection, critical
<i>cd</i>	conduction, fouling
<i>cs</i>	cross-section
<i>cv</i>	convection
<i>dg</i>	deposit, gas side
<i>dw</i>	deposit, waterside
<i>f</i>	dry fuel, fin, final, fouling
<i>f,x</i>	fin, x-direction
<i>f,y</i>	fin, y-direction
<i>fg</i>	flue gas
<i>g</i>	gas, gas side, moist air
<i>h</i>	hydraulic
<i>i</i>	inner, inside
<i>o</i>	outer, outside
<i>p</i>	particle, pipe, perforation, plate
<i>pl</i>	plate
<i>pr</i>	primary
<i>r</i>	row, radiation
<i>rb</i>	rows in a baffled zone
<i>s</i>	solid, surface, start
<i>sd</i>	surface, fouling
<i>se</i>	secondary
<i>sg</i>	surface, gas side
<i>si</i>	inner surface
<i>so</i>	outer surface
<i>sw</i>	surface, water
<i>t</i>	turbulent, fully developed
<i>th</i>	thermal
<i>v</i>	vapour, vaporization
<i>w</i>	water
<i>x</i>	co-ordinate
<i>y</i>	co-ordinate

Superscripts

<i>ep</i>	end of the plate
<i>f</i>	fin
<i>m</i>	constant
<i>p</i>	plate

Abbreviations

Ar	argon
CO	carbon monoxide
CO ₂	carbon dioxide
DEGHEX	drying exhaust gas heat exchanger
EER	heat transfer rate by effect of entrance region
FDTFC	heat transfer rate by fully developed turbulent flow
FGHEX	flue gas heat exchanger
H ₂ O	water
MC	moisture content
N	nitrogen
O	oxygen
RH	relative humidity

1. INTRODUCTION

Scope

This study introduces two methods of drying biomass for the boilers. The first one dries biomass for the use of the boiler plant itself and the second one also dries it to the market. When burning wooden biofuels in small-scale boilers one problem is moisture and its variation. The boiler plants provided with a dryer are most useful as they create new possibilities to expand the exploitation of pro-environmental fuels. The latter, *i.e.* the method of drying bio fuel to the market in connection with district heat production, gives advantages to end-users and the production plant.

Combining a dryer with the boiler plant makes the system complex. In addition to the dryer, a minimum of one heat exchanger is required. Design parameters, such as heat demand for the boiler, outdoor air temperature and moisture content of fuel vary such an extent that the designer of this kind of a system faces the following questions: What are the critical combinations of input parameters in dimensioning? Which type of heat exchanger is suitable for flue gas or for drying exhaust gas as the primary flow? How to dimension the boiler, dryer and heat exchangers considering their operational interdependencies? Modelling is needed for predicting the thermal behaviour of this complex system. This study develops and uses models that improve understanding of the thermal performance of the main components of a boiler plant equipped with dryer. Modelling also helps evaluate the usefulness of different construction alternatives for the main devices. It helps to size them, to search for suitable operation parameters and to understand interdependencies between the boiler, dryer and heat exchangers.

The devices and fluids related to this study are shown with grey raster in Fig 1. Also, the other most common drying media and heat sources for the air are shown. This study is about a cross-flow type convective moving bed dryer using warm air as a drying medium. The bed is vertical and the fuel flows down gravitationally. The air is heated either with boiler water or flue gas. When it is heated with flue gas, the air is pre-heated with heat from exhaust drying gas. Besides drying air, it is also possible to heat combustion air by this arrangement. A pipe-bundle heat exchanger is used with flue gas and a flat plate heat exchanger with exhaust drying gas. The usability of counter-, cross- and parallel-flow type of heat exchangers is analysed. The boiler under study is of a grate type. The convection part of the boiler is analysed. Two types are included, one with round tubes and the other with rectangular ducts containing an array of longitudinal rectangular fins.

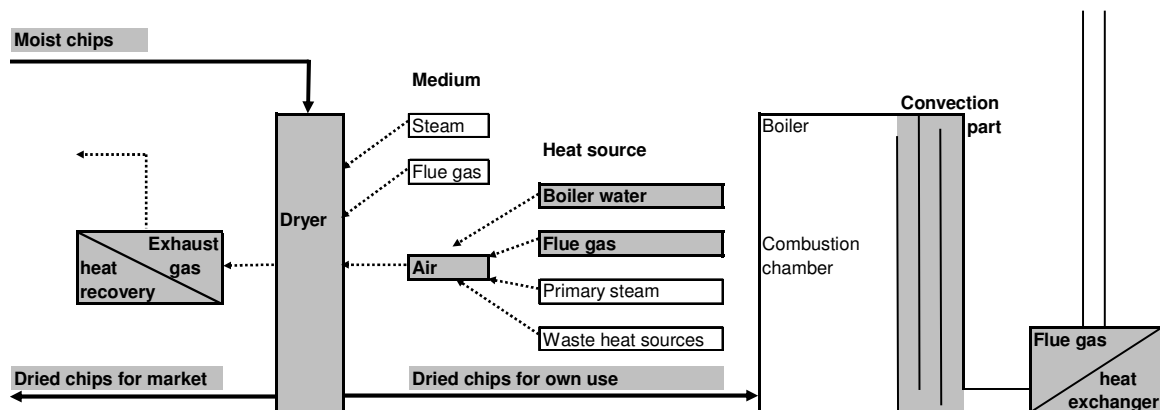


Figure 1. Boiler plant system with dryer and heat exchangers.

The dimensioning process of the equipment in a boiler plant is shown in Fig. 2. The topics which are discussed in this study are shown with grey raster. Energy and mass balance models give useful information of the boiler system. Two auxiliary models are needed with the energy and mass balances models. These models and their sources are:

- Properties of gas mixtures [1]
- Mass and energy balance of combustion [1, 2, 3]

They are based on the methods described in handbooks; hence, they are not described in this study. Energy and mass balance models are a prerequisite for the models to dimension the heat and mass transfer area. Two other auxiliary models are also needed:

- Heat transfer in the combustion chamber [1, 4]
- Pressure drop of flow [1, 5]

For brevity, these auxiliary models are not described in the review.

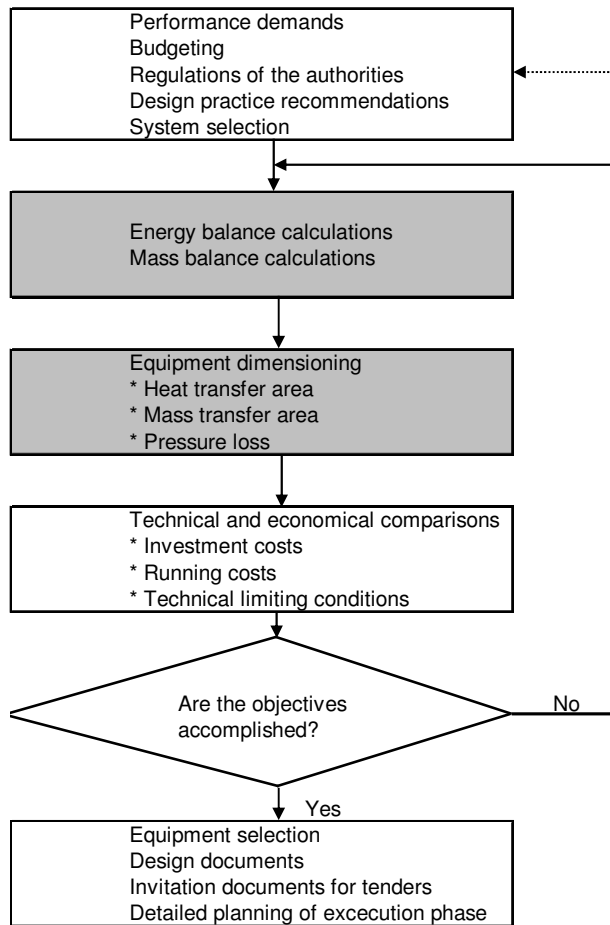


Figure 2. The progress of design process of the boiler plant.

Background

There is an increasing consensus that the activities of man are contributing to the green house effect, hence resulting in an unfavourable impact on the environment. In the production of energy, the portion of wood-based fuels has grown and will grow because of their large CO₂-neutrality. This makes the low-quality fuels an increasingly interesting potential resource also in the small-scale heat production. The Ministry of Trade and Industry in Finland has set an expansion goal of 300 % for the use of forest chips from the year 2002 to the year 2010 [6]. Forest residue is available from clear-cut final felling at a most reasonable price. This fraction is widely used in power plants and in large-scale district heating boilers. However, the challenging expansion goal also requires harvesting a large amount of whole-tree and stem-based chips from thinnings. These fractions are more expensive and therefore better suited for local small-scale heating purposes at a relatively short transportation distance. The scope of this study is on this scale. Grate firing is common in boilers of this scale, *e.g.*, in large public buildings like nursing homes, offices and schools, or in small district heating networks. The increasing use of forest chips shall also expand market for grate firing boilers.

Moisture content (MC) is one of the main concerns about the combustion of wood chips in the grate boiler plant [7]. The MC of the fresh forest residue may exceed 60 % (wet basis) in clear-cut storages in Scandinavia during winter [8]. On the other hand, with the transpiration drying method it may fall below 30 % in favourable drying conditions [9]. In the timber and carpentry industry the moisture content of by-products may be less than 10 %. Moisture needs to vaporize in the combustion chamber, and hence MC affects the construction and size of the boiler. The other two dimensioning parameters are the outdoor air temperature and the heat demand of the heating network. Outdoor air temperature varies from about -30 to 30°C in Southern Finland during the year. It affects directly the heating demand of the combustion air and the heat losses of the boiler house. If the boiler plant is equipped with a warm air fuel dryer, the effect of outdoor air temperature on the internal energy consumption increases drastically. Outdoor air temperature also affects the heat demand of the heating network. In summer, heating power may be needed only for producing warm tap water and covering heat losses in the pipe network. During the low consumption period of water, this heat load is insignificant in comparison to the load required for space heating on the coldest days. A typical guarantee value for the load variation of the grate firing boiler is 20 - 100 % in unmanned operation. A practical lower limit of 30 % of the peak load on the high quality performance is reported in Sweden [10], even though the boilers often operate at a lower load. The large range of these three dimensioning parameters (MC of fuel, outdoor air temperature and heating load) combined with the increasing requirements for efficiency, clean combustion and reliability make the design of a boiler plant challenging.

To get more homogeneous fuel, moisture content may be lowered by storing the fuel outside before delivering it to the boiler. In the Scandinavian climate, drying the residue in the clear-cut storages or landing storages needs at least one summer season and even then the result depends on the temperature and relative humidity of ambient air and precipitation, among other things. Further, the foliage and needle content decrease, which causes dry matter loss. The shedding of foliage and needles is often good from the viewpoint of soil nutrition, such as peat land forestry in particular. There, the nutrition decrease is critical to annual growth and it is possible to compensate for it by returning the ash back to the forest when collecting fresh residue. Mineral land forestry is more problematic because the lack of nitrogen limits annual growth. In combustion, nitrogen is released into the atmosphere and the benefit of returning ash decreases [9]. Another possibility is to dry chips in piles or bins, for example. With this drying method, the volatile hydrocarbons are emitted into the air in gas phase and leached into the ground by precipitation [11]. Also respiration of living cells and the metabolic rate of microbes lead to dry matter loss. The amount of such dry matter loss is not yet well known as for drying the forest residue in landings or clear-cut storages, but obviously it is smaller than in the case of drying chips. The transpiration drying method is especially advantageous in spring and in summer because it decreases rather rapidly the amount of water available for the living cells and organisms.

An alternative and complementary approach is to dry chips with special drying equipment. The drying media may be such as unheated outdoor air, flue gas, hot air or steam, and there are numerous solutions for the construction of the dryers [12, 13, 14]. Drying decreases biological degradation of the fuel and increases the heating value of bio-fuel. In some cases it is possible to use waste heat for drying. It is estimated that waste heat drying could result in a 25 % increase of the bio fuel potential in the forest industry in Sweden, without resorting to cutting more wood

[14]. If the increasing use of bio fuel compensates for the use of fossil fuels, drying has a favourable impact on the CO₂ emissions. A bio energy combine concept is suggested for upgrading fuel by drying in the context of CHP plants. In this concept, the CHP plant is integrated with pellet production [15].

Wood chip boiler plants with external dryers are still an exception. A common solution is to dry fuel inside the boiler on the grate. However, in a small-scale there are plants designed for either dry or wet chips, but not for both. If the boiler plant is equipped with an external dryer, the fuel supplied into the boiler may be homogenous even if the MC of the fuel as received varies greatly. Convection drying is the most common biomass drying process [16]. Bed drying is evaluated to be the most suitable technology for wood based bio-fuel both from the technical and commercial point of view [14]. The drying air temperature should be under 100 °C, if the exhaust gases from the dryer are released into the atmosphere [17]. This is due to the hydrocarbon emissions, which increase rapidly, if the drying temperature increases [18]. Drying of porous material has been extensively researched, but calculation comparisons with experimental results concerning deep bed drying of the wood chips have rarely been presented.

The heat transfer problem from single-phase flue gas to boiler water through the walls of the round tubes is a classic one. Heat transfer correlations based on laboratory measurements are widely published and available [1, 19, 20, 21]. Aung, Kakac and Shah have extensively summarized the previous work in [22] and Aicher and Martin have proposed a method taking into account the effect of natural convection [23]. The effect of the entrance region based on the laboratory experiments is discussed in several sources [1, 19, 20, 21, 24, 25]. However, implementing the correlations to describe the performance of the whole equipment adapted for a specific purpose with large operational range requires experimental work. The experiment result of the biomass boilers are shown in [26].

Besides the tubes another common construction of the convective heat exchange section consists of a rectangular duct with an array of longitudinal rectangular fins for flue gas and a smooth outside surface for water. Many researchers have studied the thermal performance of extended surfaces during the past eight decades. In [27] and [28] previous studies are summarised in the context of defining the optimum dimensions of different fins. In the literature, the calculation of a finned surface is presented for a clean fin [19, 20, 21, 29]. Fouling from a gaseous stream has, however, a significant effect on the energy efficiency of the boiler [30]. The heat transfer surfaces of the convection section are inclined to fouling because of the fly ash and soot on the flue gas side and because of the boiler scale on the waterside. Fouling reduces heat transfer because the thermal conductivity of ash, soot and boiler scale is lower than that of steel. Therefore, a simplified calculation of the heat transfer rate for a fin element with a fouling layer is needed. Further, an assumption of equal temperature of the plate and the base of the fin is usually applied, even if its verification is not considered.

The content of chapters

Chapter 2 describes the sizing strategy of the biomass boiler and the effects of fuel moisture on the performance of the boiler. It is shown that the heat produced by the base load biomass boiler may actually decrease even if its maximum heat power increases. The amount of the energy

produced by the biomass boiler depends on the share of the peak load and also on the minimum available load of the boiler. It is also shown that the oxidation time increases drastically if the temperature of the combustion chamber goes below approximately 750 °C. The two above-mentioned alternatives of boiler plants with a dryer are introduced. The energy and mass flows of the plant, which produces chips also to the market, are discussed. The idea to use the reserve heating effect for drying is the principal technical novelty of this study.

Chapter 3 discusses the construction, operation and modelling of the cross-flow type convective warm air dryer. Two models are described, the simplified energy and mass balance model and the deep bed model. With the former the power demand at different stages of drying icy wood chips is calculated. The deep bed model is based on the shrinking core single particle model developed by Jaakko Saastamoinen [31] and improved by him in Paper II. The single particle model is implemented into the model of the deep bed. Then the drying bed is divided into computational cells for which the mass and energy balances are solved numerically. The profiles of MC and temperature of the fuel as well as RH and temperature of the drying air are calculated with this model.

Chapter 4 concentrates on the convection section with tubes and the rectangular convection section with fins. It appears that the results of the model and measurements differ significantly if the ratio of tube length to inner diameter is small. The most probable reason is assumed to be the inaccuracy in the correlation of the entrance region. A model for the fouled fin is described. Both convection sections with tubes and with rectangular finned flow channels are analysed with the models. The effects of the design parameters are illustrated with graphs.

In Chapter 5 two heat exchangers are described and modelled, a pipe-bundle type flue gas heat exchanger and a flat plate type drying exhaust gas heat exchanger. Fouling is detected as a major problem with the flue gas heat exchanger, especially if the water vapour in flue gas condenses. Condensation is unavoidable with the counter flow type, and the heat output of a parallel flow type is insufficient. Therefore, a type where cross-flow elements are arranged as mixed-flow is found applicable. Fouling is a problem also with the heat exchanger recovering heat from dryer exhaust gas. Therefore, a dust collector between the dryer and the heat exchanger is needed. A parallel flow heat exchanger type is found most appropriate for the heat recovery heat exchanger. With the parallel flow type no risk of freezing occurs.

The Papers are prepared within a rather long period in context of three different projects with different aims and partners. Therefore also the method of treatment differs in Chapters. The model of convection section, for example, is explained more detailed than other models because the aim of the respective project was to achieve a dimensioning tool for boiler designers.

The energy and mass balance as well the bed models for a dryer have been verified by measurements conducted in the laboratory test rig at Satakunta University of Applied Sciences. Tests were performed with varying heights of the fixed bed, wood species and initial MC and drying air temperature and velocity. Long-term practical operation results were collected in a 40 kW_{th} pilot plant in Nakkila and in a 500 kW_{th} demonstration plant in Kullaa. A model for the convection section with tubes was verified by laboratory measurements of the 50 kW_{th} pellet boiler in the laboratory of the manufacturer in Saarijärvi and by field measurements of the 4000

kW_{th} wood chip boiler in Suomussalmi. A model for the finned convection section was verified by laboratory measurements of the 300 kW_{th} wood chip boiler in the laboratory of VTT in Jyväskylä and by field measurements of the 500 kW_{th} demonstration plant and 1000 kW_{th} wood chip boiler in Vierumäki. A model for the tube-bundle type flue gas heat exchanger was verified by measurements on the 40 kW_{th} pilot plant and the 500 kW_{th} demonstration plant. A model for the flat-plate type exhaust drying air heat exchanger was verified by measurements on the 500 kW_{th} demonstration plant. All results of the experiments are described in Papers I...III and V...VI. Only the results of the measurements for the convection section are shown in this review. This is because the model of it was the only one, indicative of a significant difference between the results of the model and those of the measurements. All other models gave results in reasonably close accordance with the verification measurements.

2. BIOMASS BOILER PLANT

2.1 Design aspects of the boiler plant

Sizing of the boiler

In Finland the duration of very cold outdoor air temperature is typically short. The share of the annual energy use during the high heat demand period is small. Also, grate fired boilers are more expensive than light oil boilers, for example. In consequence, a grate-fired biomass boiler is often dimensioned for the base load whereas a light oil boiler is chosen as a peak load and a standby boiler. The share of the peak load is often approximately 40 - 60 % for a grate fired boiler, and its share of the total produced energy does not notably increase, even if its share of the peak load increases. On the contrary, it may even decrease, see Fig. 3.

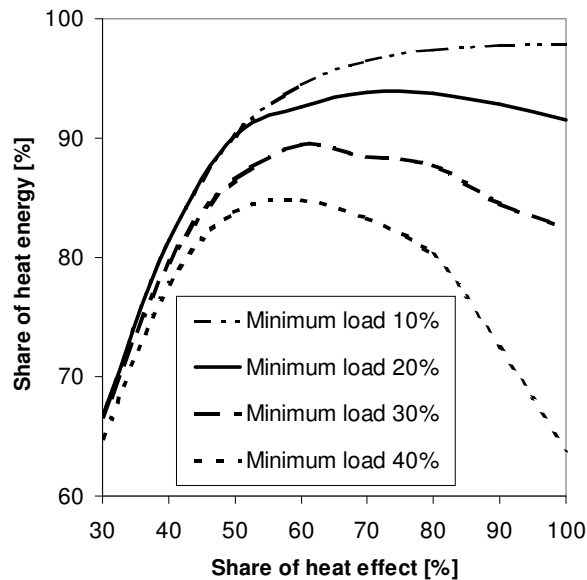


Figure 3. The share of produced energy as a function of the share of heat effect and minimum heat load as a parameter (Paper IV).

Figure 3 is calculated on the basis of heat demand duration typical of a small district heating network in Finland. Here the minimum load for a biomass boiler stated in the warranty clause is often approximately 20 %. It is difficult to spread a small amount of fuel evenly on the grate and to achieve a good mixing of a small amount of combustion air with pyrolysis gases. These problems result in incomplete combustion and low efficiency. A practical limit of 30 % of the peak load on the high quality performance is reported in Sweden [10]. There is also a fire risk during a very low load.

Effects of moisture in the fuel

Figure 4 illustrates the effect of moisture content (MC) in fuel on the efficiency of the boiler. The result is based on the energy balance calculations. The higher the MC is the lower the adiabatic

combustion temperature is and the higher the mass flow rate of flue gas. Thus, the heat output and the efficiency of the boiler decrease with increasing MC. However, if the outlet temperature of the flue gases is below the dew point of the water vapour, the efficiency calculated in accordance with the LHV (lower heating value) of the fuel begins to increase, when the MC increases. This is because the water vapour of the flue gas condensates and releases heat into the boiler. The turning point of the efficiency curve shows the dew point temperature of the flue gas. In the example in Fig. 4 the combustion air temperature is 0 °C, relative humidity of the combustion air 60 %, excess air ratio 1.4 and dry fuel composition $\text{CH}_{1.466}\text{N}_{0.009}\text{O}_{0.633}$. Similar calculations are presented in [32, 33].

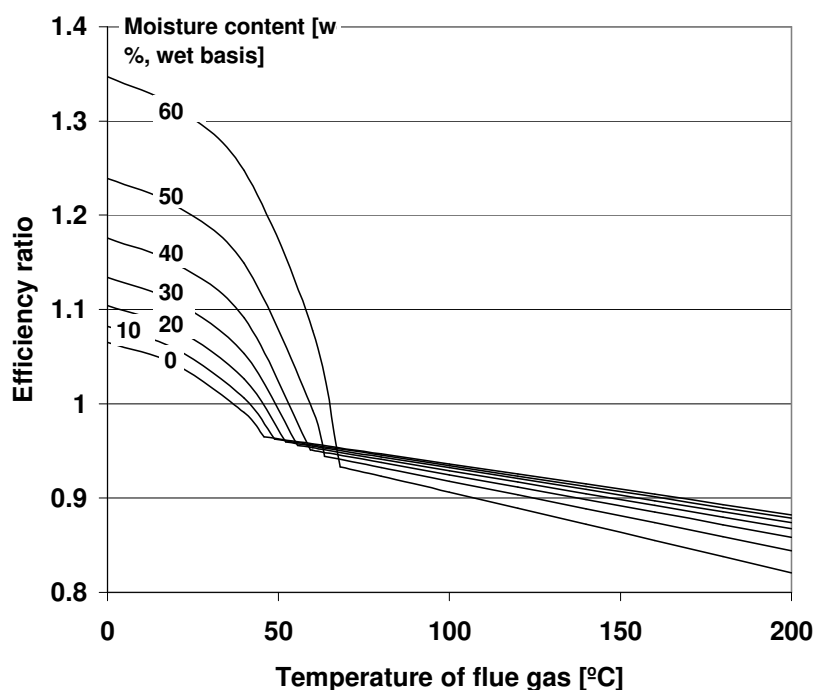


Figure 4. Efficiency ratio depending on the flue gas temperature and moisture content of the fuel (Paper I).

The temperature of the combustion chamber decreases, if the MC of the fuel increases because energy is needed to evaporate water. Further, to remove the evaporated water a higher flow rate of primary air is needed which cools down the chamber. The temperature drop has disadvantages as for the thermal performance and emissions of the boiler.

In Fig. 5 on the left is shown the construction of the grate-fired warm water boiler. On the right are shown O_2 and H_2O concentrations and the computational temperature, T_1 , in the lower part of the combustion chamber. The gas phase CO oxidation rate during combustion depends on the temperature and the CO, O_2 and H_2O concentrations in the combustion chamber [34]. In Fig. 2.3 on the right are shown the temperature, T_2 , and the CO oxidation time in the upper part. If the CO is not totally oxidized in the lower part of the combustion chamber because of insufficient mixing or delay time, the oxidation time increases strongly in the upper part combustion chamber when the moisture content of the fuel exceeds 50 %.

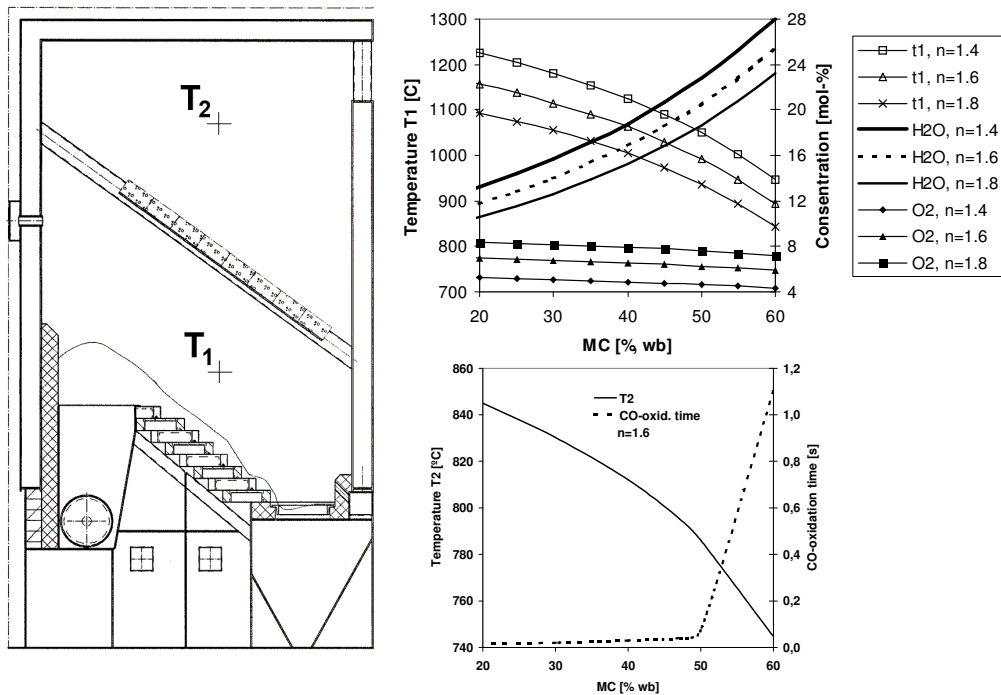


Figure 5. The construction of a grate firing boiler, 99 % oxidation time of CO and the parameters affecting it (Paper IV).

The initial volumetric concentration of CO in the calculations is 0.5 % and the final one 0.005 %. A completely mixed flow in the upper part of the combustion chamber is assumed. The oxidation time is calculated with the method described in [34]. The mean temperatures in the lower and upper parts of the combustion chamber are calculated with the method described in [1]. If the mean temperature is lower than 800 °C the oxidation time begins to increase rapidly, and if the temperature is lower than 740 °C the oxidation time exceeds the delay time in the upper part of the combustion chamber of the boiler under review.

2.2 Biomass boiler plant with dryer and heat exchangers

2.2.1 Drying of fuel for the own use

Problems due to high MC of the fuel are avoidable if the boiler is equipped with a dryer that operates in parallel with the boiler, see Fig. 6. Three additional components are needed: a flue gas heat exchanger, a drying silo and a heat recovery heat exchanger for the exhaust gas of the drying silo.

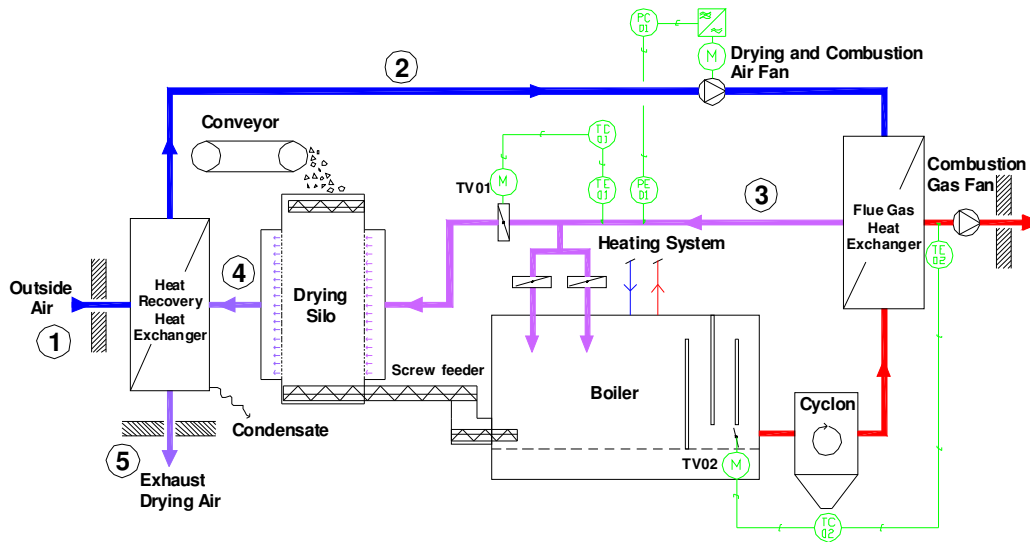


Figure 6. A schematic diagram of the boiler plant with the dryer (Paper III).

The drying air is heated in the recuperative heat exchanger using the heat of flue gases. Then, hot air is blown through the fuel bed in the drying silo, where the fuel dries, and the air cools and is humidified. The heat of the exhaust air from the silo is recovered for preheating the drying air and for combustion. This is beneficial because the enthalpy of the exhaust air from the drying silo is high. The boiler is an ordinary warm water boiler designed for dry bio-fuels. The drying air temperature is kept at the set value by regulating the flue gas cooling effect and the volume flow rate of drying air. The control strategy is described detailed in Paper III.

2.2.2 Drying of fuel for market

An alternative approach is to dry fuel not only to own use but also to the market. The degree of upgrading the product increases when the fuel is also sieved. A maximum heat effect is needed for a short time while the rest of the time reserve effect is used to dry the fuel. The principal schema of the boiler plant with a dryer and a sieve is shown in Fig. 7. The dryer is connected in parallel with the heating network. The fuel used in the boiler is a mixture of wet unsieved chips and dry reject fraction from the sieve.

This kind of arrangement gives farmers or other members of energy co-operatives, for example, a chance to earn extra income. One large boiler using low quality fuel produces high quality fuel for many small-scale boilers. The load of a large boiler is more stable than that in the traditional district heating use. Therefore, controlling of the combustion is improved and the problems of a minimum load use are avoided. This method has also indirect advantages. It brings savings in investments, because the boilers of small-scale users can be designed smaller and simpler due to the high quality of fuel. The grate area and the volume of combustion chamber decrease. The higher the temperature of the combustion chamber and combustion gases are, the smaller the heat transfer surface area needed in the boiler. Homogenous fuel enhances possibilities for accurate

control of combustion, which improves the efficiency and reduces pollutant combustion emissions from the small boilers.

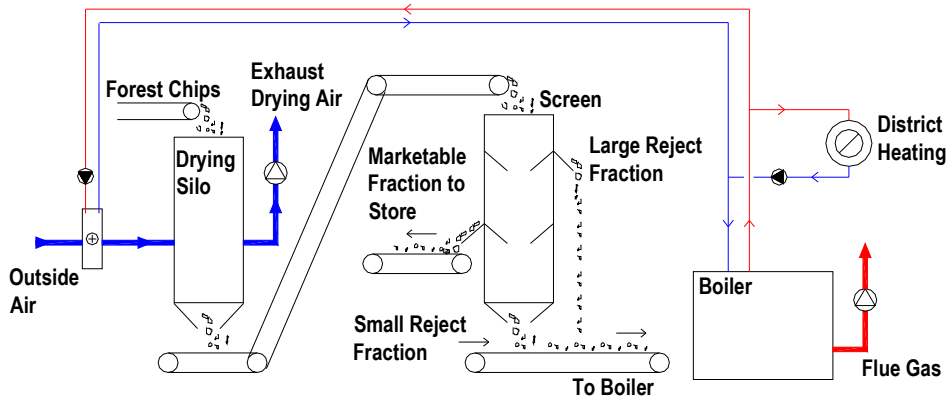


Figure 7. Principal schema of the dryer and sieve in a boiler plant (Paper IV).

Fig. 8 shows the energy available for drying chips to the market. Availability depends on the share of the biomass boiler effect and on the dimensioning of the dryer. The maximum heat demand of the network is 1 MW.

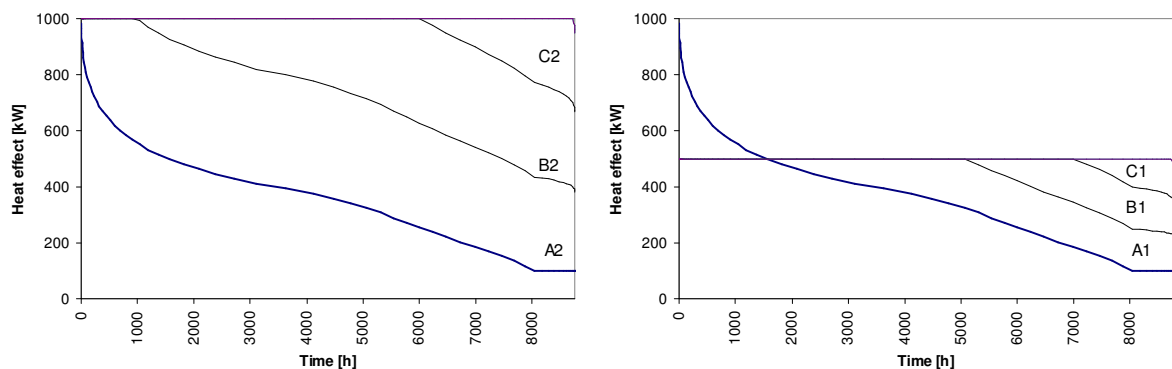


Figure 8. Heat demand of the heating network and the dryer depending on the dimensioning of the dryer. The boiler is dimensioned for the peak load of the network (on the left), or for a half of it (on the right) (Paper IV).

More detailed information about the mass flow rates and main components of the system are shown in Table 1.

Table 1. The volume flow rate of chips, mass flow rate of drying air and basic information of drying air fan and drying silo. The numerical values on rows A1 – C1 differ from those in Paper IV where they in error represent values of drying air temperature 70 °C.

	Wet chips		Dried chips	Drying air	Fan	Drying silo	
	Incoming m ³ /a	Own use m ³ /a	To market m ³ /a	Mass flow rate kg/s	Power kW	Energy MWh/a	Face area m ²
A1	7827	5683	2144	1.8	1.9	10.0	3.8
B1	11790	6332	5458	3.6	3.8	13.9	7.6
C1	13136	6541	6594	5.4	5.7	13.7	11.3
A2	25433	9497	15936	4.0	4.3	35.8	8.5
B2	41988	12443	29545	8.0	8.5	53.9	17.0
C2	46022	13082	32940	12.1	12.8	51.1	25.5
A2*	30367	10681	19686	7.7	7.4	59.1	14.9
B2*	43108	12873	30235	15.3	14.9	72.5	29.8
C2*	44388	13067	31321	23.0	22.3	62.5	44.6

* Drying air temperature 70 °C

The MC of incoming fresh forest chips is assumed to be 50 %, drying air temperature 100 °C (besides the cases marked with *). Chip amounts are expressed in units of loose-m³. The density of dry material is assumed to be 150 kg/loose-m³. The amount of reject depends on the raw material and on the properties of the chipping machine. It has to be deducted from the amount of dried chips to the market. On the other hand, this reject reduces the incoming mass flow of wet chips because the boiler uses this residue fraction itself.

2.3 Discussion

It is well known that because of the high investment cost a biomass boiler is often dimensioned for the base load. However, in Fig. 3 is shown that purely from the point of view of maximum energy production, the optimal share of the peak load is 60 - 70 %. This is, when the minimum load is 30 – 20 % of the peak load. The energy share of the biomass boiler is then 89 - 93 %. With the approach in Fig. 3 it is possible to get an estimation of additional bio-fuel use if the minimum load decreases.

Increasing MC may increase CO₂- emissions as shown in Fig. 4. It also increases primary combustion air flow due to drying the fuel. With a higher primary air flow rate, also the NO_x emissions tend to increase [35]. On the other hand, the increasing air flow rate cools down the combustion chamber. This may decrease thermal NO_x. Decreasing NO_x emissions have been measured with the increasing fuel MC [36].

A screw feeder or hydraulic pushing chutes supply fuel to the boilers with an inclined grate. The height of the fuel bed is adjustable. The grate is subdivided into equally sized steps. In small boilers and with reasonably homogeneous and dry fuel, fixed grates are used where fuel flows downwards gravitationally, see Fig 5. In travelling grates every second step is fixed while the steps in between move forwards by means of hydraulic pistons pushing fuel over the edge to the next step. The ignition front has been assumed to take place at the surface of the bed by radiation from flames and refractory surfaces above the bed. However, it has recently been shown that the ignition front locates more probably at the surface of the grate [37]. When the boiler begins to receive wetter fuel, the combustion temperature and the rate of propagation of ignition on the grate decrease. This is valid regardless of the location of the ignition front. According to measurements for wood chips and peat the grate area required for complete combustion increases by approximately 120 % when the moisture content of the fuel increases from 30 to 60 % [38]. If combustion air temperature increases, the propagation velocity of the ignition front in the fuel bed and the heat effect of the boiler increase.

Table 1 shows useful interdependencies in the system design. Firstly, the amount of chips to the market increases with the increasing drying air mass flow rate, but not linearly as in the case of the fan power and dryer face area. The amount of marketable chips grows from 65 and 85 % when the capacity of the dryer increases by 100 % (i.e., from one third to two thirds of the full capacity), in other words from case A1 to B1 and from A2 to B2, respectively. With an equal increase in capacity from B1 to C1 and from B2 to C2 the growth is only 9.6 and 11.4 %, respectively. On the other hand, compared to the incoming amount of chips the share of marketable chips increases with the increasing drying capacity. This is because with the greater drying capacity the use of drying energy is emphasized during the warm season. The same feature relates to the drying air fan. Even if the size of the drying air fan increases linearly with the increasing capacity of the dryer, the need for a fan energy does not. This is because the greater the capacity of the dryer is the longer the time the fan operates at a partial load. It is possible to optimise the capacity of the dryer taking into account the investment costs. Secondly, drying also enables the biomass boiler to take an increasing share of the peak load. The problem of a minimum load can be avoided by using the energy for drying in summertime. This is profitable because the specific heat demand is relatively low during the warm season and oil can be replaced with the cheaper biomass in the case of an oil-fired secondary boiler. Therefore, the size of the biomass boiler can be included in the optimisation. Thirdly, modelling gives possibilities to study the effects of changing operational parameters. Contrary to expectations, decreasing the drying air temperature from 100 to 70 °C may increase the amount of marketable chips. For instance, in the case of one third of the full capacity (from A2 to A2*) the increase is 23.5 %. From the point of view of dimensioning the components there is also an optimum for the drying air temperature. When increasing drying air temperature the needed size of the heat exchanger increases. On the other hand the drying time and the subsequent size of the dryer decrease.

3. DRYER

3.1 Modelling

3.1.1 Energy and mass balance model

The dryer is a cross-flow type convective warm air bed dryer, see Fig. 9. The fuel is led into the drying silo by a conveyor and spread evenly by a screw. Then the fuel flows down gravitationally and is led into the boiler by the screw feeder. The cross-section of the silo is rectangular and the longer sides are constructed from a perforated plate with small holes. The hot drying air is blown through the holes and the fuel bed. The water vapour evaporating from the fuel particles cools and humidifies the drying air so that it is almost saturated when leaving the silo. The construction of the silo is based on the experimental study concerning the 40 kW_{th} pilot plant, where several alternatives were investigated [39].

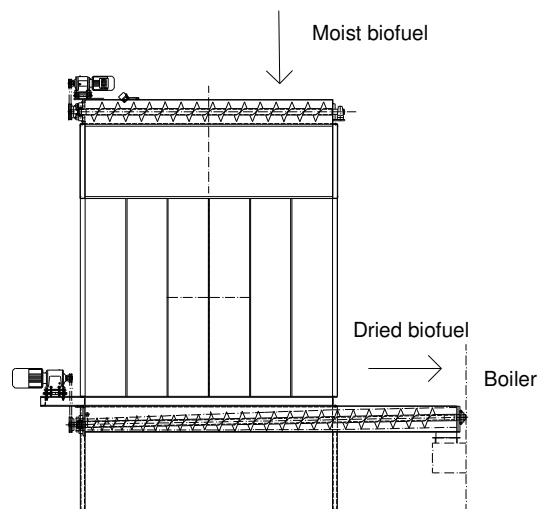


Figure 9. Scheme of the drying silo in the demonstration plant of Pori Forest Institute (Paper I).

The modelling of the silo is simplified so that heating and melting the ice, heating the particles and evaporating the water are assumed to be successive. In reality these stages are partly simultaneous because of the different sizes of particles and the cross-flow type of the silo. Small particles may be almost dry while the large ones still include water. Particles may be almost dry near the surface while they might be still icy in the middle. In the front of the silo the particles are dry while in the back they still are icy or moist. During the stages of heating and melting the silo is treated like a heat exchanger. During the stage of evaporation the exhaust air is assumed to be saturated. The structure of the dimensioning model is shown in Fig. 10.

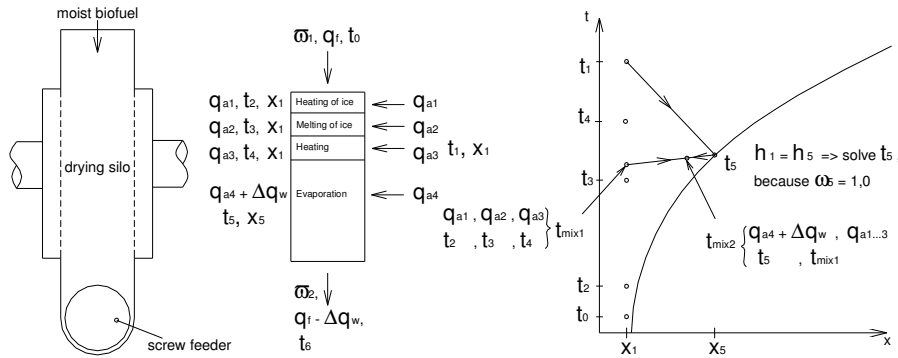


Figure 10. The principle of dimensioning calculations of the drying silo (Paper I).

The mass flow rates $q_{a1} \dots q_{a3}$ of the air needed for heating and melting the ice, heating up the wood and remaining water to the final temperature (t_6) are achieved by means of energy equilibrium calculations, using the mass flow rate, initial and final moisture content (ω_1 and ω_2 , respectively) and temperature of fuel as input data. The mass flow rate of air (q_{a4}) needed to evaporate the water (Δq_w) is calculated by assuming the outlet air of the evaporation stage saturated (ϕ_5) and the state of the drying air changing along the curve of constant enthalpy. The total mass flow rate of the air needed is the sum of the mass flow rates of different stages added with the mass flow rate of evaporated water. The outlet temperature of the air (t_{mix2}) is the mixing temperature of the outlet temperatures of different stages.

3.1.2 Modelling of the deep bed

The silo is divided into small computational cells, for which the mass and energy balances are solved, see Fig. 11. The output values of one cell are input values for the next cell. The heat and mass transfer rates are calculated using the Single Particle Model in Paper II. The gas flow is assumed one-dimensional; the ratio of the particle size to the length of the test rig test was small and the bed sufficiently deep. The plug flow assumption is applied. Fuel homogenisation before feeding to the dryer is needed to avoid lumps causing channelling of the gas flow. The heat conduction, diffusion and mixing in the flow direction is assumed negligible in the bed in comparison with the convective flow. In cross-flow the vapour from drying the particles will cause some distribution in the gas mass flow rate, but the deviation from one-dimensional assumption is small.

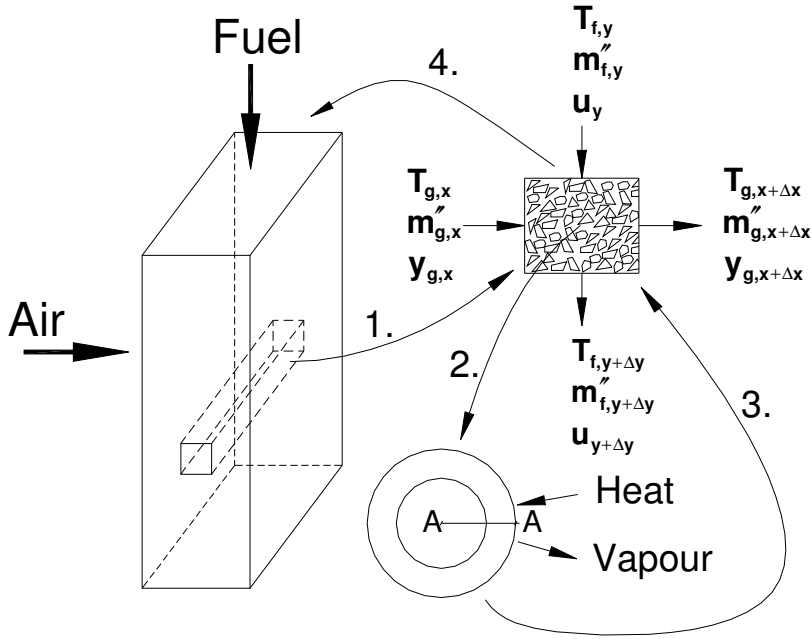


Figure 11. Procedure and notes of the deep bed modelling (Paper II).

The procedure of modelling is: 1. The silo is divided into small computational cells, 2. The heat and mass transfer rates are calculated for one spherical particle in the middle of the cell. 3. The heat and mass transfer rates for a single particle are combined with the heat and mass balance of the cell and solved numerically, 4. The output values of one cell are input values for the next cell, and no iterative calculations are needed due to the cross-flow principle of the dryer.

The moisture balance between fuel and air in the cell is given by, when $\Delta x, \Delta y, \Delta z \rightarrow 0$

$$\dot{m}''_{g,x} \frac{\partial Y}{\partial x} = -\dot{m}''_{f,y} \frac{\partial u}{\partial y} = \dot{m}''_s S'' \quad , \quad (1)$$

The term on the left describes the change in moisture content of the drying air flowing through the cell. The term in the middle shows the corresponding change of the moisture content of the fuel while the term on the right expresses the evaporation mass flow in the cell. In Paper I this is treated in a simpler way using empirical function based on the laboratory measurements

The total energy balance of the cell for $\Delta x, \Delta y, \Delta z \rightarrow 0$, yields:

$$\dot{m}''_{g,x} \left(c_a \frac{1-2Y}{1-Y} + c_v \frac{Y}{1-Y} \right) \frac{\partial T_g}{\partial x} = \dot{m}''_{f,y} (c_f + uc_w) \frac{\partial T_f}{\partial y} + \dot{m}''_{g,x} \left(l_v + c_v \frac{Y}{1-Y} (T_g - T_f) \right) \frac{\partial Y}{\partial x} = h_c S'' (T_g - T_s) \quad (2)$$

The term on the left describes the decrease in the sensible heat of the flowing air and the first term in the middle shows the increase in the sensible heat of the fuel. The second term in the middle consists two parts: the energy needed for the evaporation and the energy needed to heat

the evaporated amount of water from the fuel temperature to the air temperature. The term on the right expresses the rate of the heat transferred from the air to the fuel particles.

The heat transfer rate is calculated in the middle point of the cell with the single particle modelling using the reported correlation [40, 41] for the heat transfer coefficient. Partial differential equations (1) and (2) are discretized and then solved numerically with the equations of a single particle. If the partial pressure of water vapour is greater in the air than at the evaporation front, the vapour starts to condensate on the surface of the particle, see Fig. 14.

In Paper I the vaporizing mass flow rate was calculated simpler by using the mass transfer coefficient k , which is yielded from the heat and mass transfer analogy and is a function of convective heat transfer coefficient α , Lewis number and exponent n . Lewis number is a quotient of Prandtl number and Schmidt number. Below the critical moisture content the rate of vaporizing mass transfer decreases due to the internal mass transfer resistance of the particle. This is tried to take into account by the function based on the laboratory measurements.

3.2 Analyses

3.2.1 Energy and mass balance

The energy demand of the heating and evaporating stages depending on the temperature of outdoor air is shown in Fig. 12.

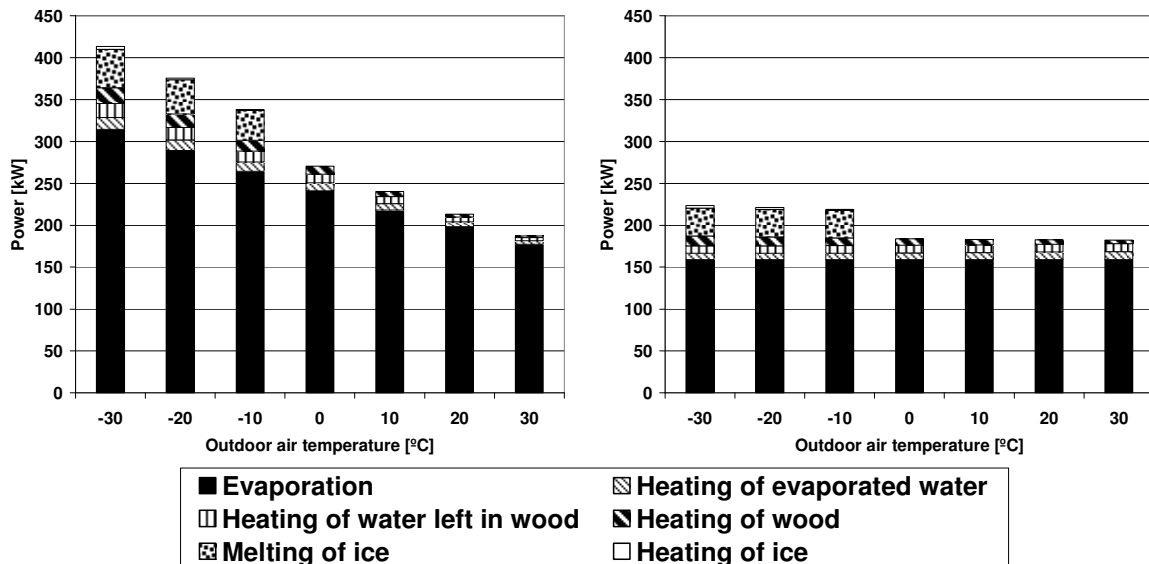


Figure 12. The components of heat power demand of the drying air in a 1 MW boiler plant at different outdoor air temperatures. The bars on the right describe the heat demand of the different stages strictly and on the left the power needed to heat up the drying air is allocated for the stages (Paper I).

No heat is recovered, the initial and final moisture contents of fuel are 60 % and 35 %, and the temperature of the drying air is 90 °C. The demand for heat at different stages changes a little, depending on the temperature of ambient air. The only greater change is at a temperature of 0 °C because of the melting heat of ice. However, the outdoor air must be heated to rather high a temperature for heating and evaporating purposes. This is why the heat demand for warming up the outdoor air strongly depends on the ambient temperature.

The influence of outdoor and drying air temperature and initial moisture content on the heat demand is shown in Fig. 13. The final moisture content is 20 %.

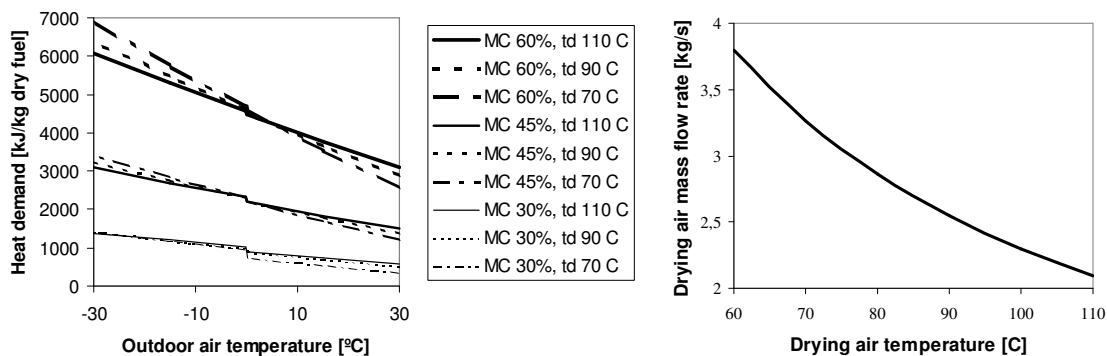


Figure 13. Influence of outdoor air temperature, initial moisture content and drying air temperature (td) on the specific heat demand of drying (on the left), and the drying air mass flow rate as a function of drying air temperature (on the right) (Paper IV).

The sorption heat is not notable because the final moisture content is near the fibre saturation point of wood. This and the heat losses of the drying silo are omitted in calculations. The outdoor air temperature is 0 °C and the starting moisture content is 45 % when calculating the drying air mass flow rate.

The influence of the drying air temperature on the heat demand is not strong, even if the needed drying air mass flow rate reduces strongly with the increasing drying air temperature. The specific energy consumption is smaller at high temperature than it is at low air temperature in wintertime, but the situation is the inverse in summertime.

3.2.2 Deep bed

Profiles of temperature of drying air and fuel particles, moisture content of fuel, and RH of drying air are shown in Fig. 14.

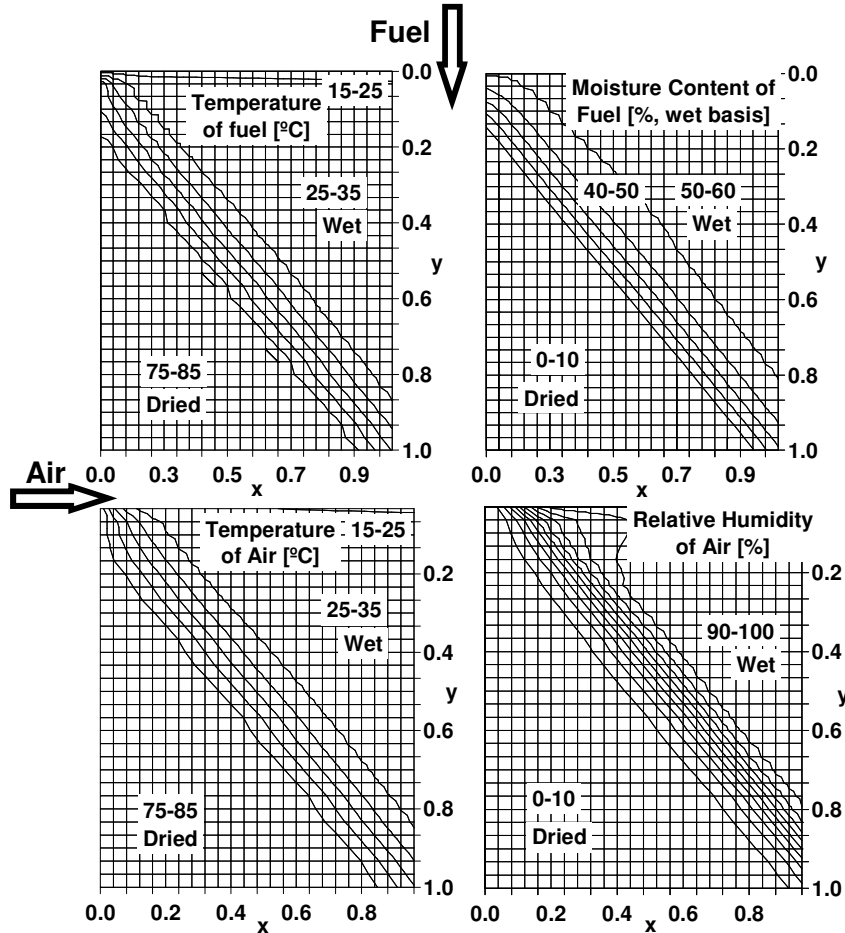


Figure 14. Scheme of changes in the moisture content ($\omega_0=51.8\%$, wb) of fuel, relative humidity ($\phi_0=2.7\%$) of drying air and temperatures of air ($T_{a,0}=354\text{ K}$) and fuel ($T_{f,0}=293\text{ K}$) (Paper II).

The values of the initial and final stages are shown and the intermediate stages are between the border lines, respectively. In the right upper corner of the silo the moisture content of wood is higher than in the beginning, because the water vapour condenses on the surface of the particle. On the other hand, particles may have very low moisture content in the lower front part of the silo. Most of the water seems to evaporate in rather a narrow diagonal area.

3.3 Discussion

Drying a fixed bed of material is clearly a two-stage process for the deep bed, if the short initial heat-up period is not considered. This can be seen in the experimental results in Paper II, and it is

illustrated more clearly in Fig. 15. At the first stage, the air outlet temperature is constant as shown by the measurements and also predicted by the model. Then air at the outlet is practically saturated and the drying rate (mass release of water from the fixed bed) is constant and the average (mixing) moisture content (dry basis) decreases linearly as shown in Fig. 15. At the second stage, the outlet temperature starts to increase and the humidity to decrease. The rate of drying decreases reaching finally the equilibrium moisture, if the drying time is long enough.

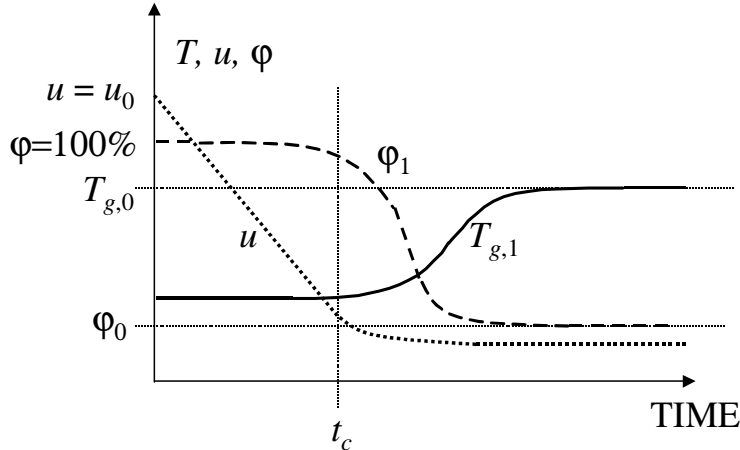


Figure 15. Temperature and relative humidity of outlet air from the fixed bed. Here, 0 and 1 denote inlet and outlet conditions, respectively (Paper II).

There are several factors that are not very well defined for wood chips used in practice such as anisotropy, cracks, size and shape distributions. How to define the size and shape of an irregular particle is also a question. Drying the fuels of different sizes can be compared by choosing a suitable size criterion such as the average shortest dimension of the particles. Another way is to reduce a particle to an equivalent sphere with a diameter $= 6 \times \text{volume/surface area}$. Then the additional heterogeneous factors are included in the effective diffusivity D_p of the fuel particles, which is not size dependent. The shape could be characterized by sphericity [41]. The future more advanced modelling could take into account the distributions in size and sphericity of the material. These simplifying assumptions may have an adverse effect on the results.

The size and shape of the chips are inherently inhomogeneous. They flow downwards by gravity in the silo the longer side of which is partly made of a perforated plate with 3 mm holes. The first challenges in developing work were to get the chips to flow evenly in the silo and to prevent vaulted cavities forming in the silo (in other words, to the plug-flow both for air and particles). If the residence time of the wood chips changes at different locations in the silo, the drying rate decreases. To reach the plug-flow satisfactorily, several improvements in shaping and modifying the silo and the screw feeder were needed.

Laboratory measurements were performed for various bed materials, bed depths, and temperature and flow rates of the drying air. The results are described in detail in Paper II. The model describes drying of the silo accurately enough for product development purposes. The calculated rate of evaporation compares well with the measurements but the air temperature differs more. In the opinion of the authors the main sources of inaccuracy of the assumptions mentioned above are the plug-flow assumption and the estimation of heat transfer area (chips treated as spherical

particles). On the other hand the thermocouples were placed inside the bed and the difference may also be partly due to inexact position of thermocouples or their attachment to particles.

4. CONVECTION SECTION OF THE BOILER

4.1 Convection section with tubes

4.1.1 Modelling

The heat transfer coefficient of the flue gas side controls the heat transfer rate of a convection section. It consists of radiation and convection, $h_g = h_r + h_c$. The radiation heat transfer is decisive in the combustion chamber, but it is less significant in the convection section. This is due to the small diameter of the tubes, a relatively low temperature, and a small amount of fly ash as well as small concentrations of emitting gas components of CO₂ and H₂O [1]. Initial and final temperatures are typically in the range of 250 - 600 °C and 100 - 250 °C, respectively. The convection heat transfer coefficient is calculated with Eq. (3)

$$h_c = Nu_k g / d \quad (3)$$

For a fully developed turbulent flow, the correlation of Petukhov, Kirillov and Popov is applied [22].

At the entrance region, the heat transfer is more efficient in comparison with the fully developed turbulent flow because of the undeveloped velocity and temperature profiles. A general Eq. (4) for the relation of the mean Nusselt number in the entrance region, $z (= l/d_i) < 60$, and the Nusselt number for fully developed turbulent flow have been presented in [19, 22]. In this study, this relation is called the Nu correction factor.

$$\overline{Nu} / Nu_t = 1 + C / z^m \quad (4)$$

The values of constants C and m depend on the configuration of the entrance. By choosing the most appropriate configuration as compared with the case of the convection section of the pellet boiler, Gnielinski proposes $C = 1$, $m = 2/3$ [24], Grass $C = 2.3$, $m = 1$ [25], Mills $C = 2.4$, $m = 0.68$ [20] and Sukomel $C = 0.83$, $m = 0.67$ ($z < 15$), $C = 0$ ($z \geq 15$) [21]. To illustrate the effect of the entrance region, these four are compared in Fig. 16.

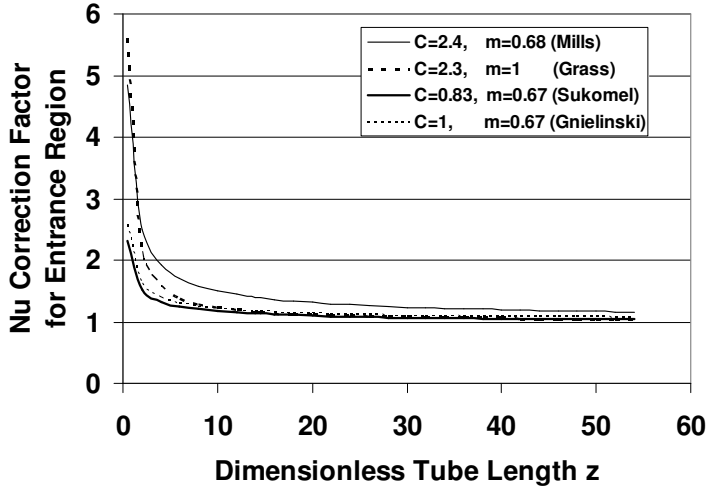


Figure 16. Mean Nu correction factor of the entrance region for turbulent flow depending on the dimensionless tube length (Paper VI).

The flue gas cools down in the convection section, and its velocity and fluid properties change all along the tube. To improve the accuracy of the model, the tube is divided into an optional number of computational cells in the direction of the flow, if needed. Therefore, the Nu correction factor is solved from Eq. (4). The mean and local Nusselt numbers are shown in Eq. (5).

$$\overline{Nu} = Nu_i(1 + C/z^m) = z^{-1} \int_0^z Nu dz \quad (5)$$

This yields for the local Nu

$$Nu = [1 + (1 - m)Cz^{-m}]Nu_i \quad (6)$$

Integrating Eq. (6) from z_i to z_{i+1} , a mean Nusselt number for each part of the tube can be calculated, Eq. (7)

$$Nu_{z_{i+0.5}} = Nu_i [z_{i+1} - z_i + C(z_{i+1}^{1-m} - z_i^{1-m})] / (z_{i+1} - z_i) \quad (7)$$

The correlation equations for laminar flow and mixed convection are shown in Paper VI.

The energy balance Eq. (8) is solved numerically.

$$-\dot{m}_g c_p (T_{g,z_{i+1}} - T_{g,z_i}) = h_g A_i (\bar{T}_g - \bar{T}_{si}) = \frac{n\pi(z_{i+1} - z_i)d_i}{R_i + \frac{\ln(d_o/d_i)}{2k_p} + R_o} (\bar{T}_{si} - \bar{T}_{so}) = h_w A_o (\bar{T}_{so} - \bar{T}_w) \quad (8)$$

The heat transfer coefficient of the waterside, h_w , is assumed constant, because it is typically one order of magnitude greater than h_g . The heat transfer resistances of the fouling layer and the heat conductivity of the tube wall material are input data. Other input data are the mass flow rate, initial temperature and composition of the flue gas. When calculating the Reynolds number, kinematic viscosity is calculated at the mean temperature of the bulk flow, while other heat transfer properties are calculated at the mean temperature of the boundary layer. The properties are calculated according to the molar composition of the flue gas with the method described in [1].

4.1.2 Experiment

The performance of the convection section of the 50 kW_{th} wood pellet boiler was measured at the laboratory of Thermia Ltd in Saarijärvi and that of the 4000 kW_{th} wood chip boiler on the Suomussalmi site in Finland. The fuel source for the latter (exp. 3 - 7) was a mixture of 60 - 80 % wood chips, 0 - 30 % bark and 10 - 20 % REF.

The measured results of the final temperature and the heat transfer rate of the convection section are compared to the predictions produced by the model in Fig. 17. The boilers were run at a constant heating load. Each of the presented temperatures is the mean value of a measuring period of 30...70 minutes.

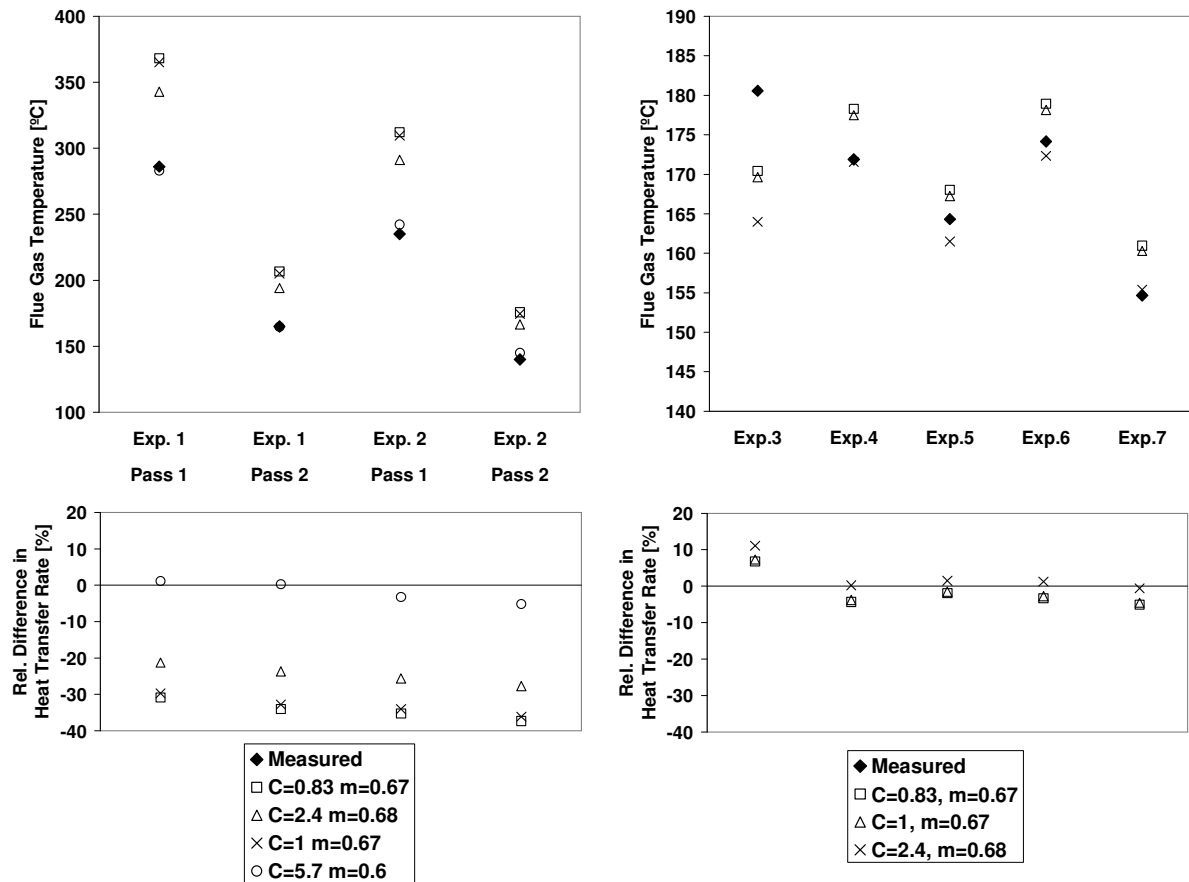


Figure 17. Comparison of measured and calculated temperatures, and relative difference between the calculated and measured heat transfer rate of the convection section. Values of the pellet boiler are on the left and those of the wood chip boiler on the right (Paper VI).

The heat transfer resistance caused by fouling is omitted from calculations because the pellet boiler was new and the wood chip boiler had recently been swept. Establishing the final temperatures and the heat transfer rates of the convection section constitute the main results of the calculations. The entrance region is taken into account in accordance with Eq. (10) where the constants, C , and, m , are defined as referred to by [20, 21] and [24], see Fig. 4.1. The dimensionless length, z , of a tube is 19.1 on the pellet boiler and 60.1 on the wood chip boiler. On the pellet boiler the calculated temperature after the first pass is 84 to 109 °C higher than the measured one and after the second pass 37 to 53 °C, respectively. The mean heat transfer rate is 37 to 44 % smaller than the measured rate, when using correlations from references [20] and [21], respectively. To correct the values of the constants in Eq. (10) they were chosen so that the mean heat transfer rate would be accurate enough in comparison with the measured values. There are several options for values C and m of which $C = 5.7$ and $m = 0.6$ were chosen. With these values the relative difference between measured and calculated heat transfer rates varied between -1.1 to 2.5 % in all cases.

Contrary to the above, the accuracy of calculations for the wood chip boiler is good. The calculated final temperatures differ by -6 to 2 °C from the measured ones in Exp. 4 - 7, and by 10

to 17 °C in Exp. 3. The calculated heat transfer rates differ by -5.1 to -1.5 % from the measured ones in Exp. 4 - 7, and by 6.8 to 11.1 % in Exp. 3. Experiment 3, which was carried out on the first day differs from the others. The experiments were performed on three subsequent days, and thermocouples were removed at the end of each day and duly reinstalled the following day. The installation may have been erroneous the first day. Nevertheless, when including all results, the mean value of magnitude of the relative difference in the heat transfer rate is 3.7 %. Therefore, no correction to the values of C and m is needed.

4.1.3 Analyses

Five analyses are described, one concerning the method itself, and four demonstrating the designer's possibilities to exploit a simulation method for optimising the construction. All analyses are calculated for the pellet boiler with a full load condition being the starting point and with constants $C = 5.7$ and $m = 0.6$.

The effect of different factors on the heat transfer is shown in Fig. 18. The effect of radiation, forced convection (fully developed turbulent flow and entrance region) and free convection are taken into account.

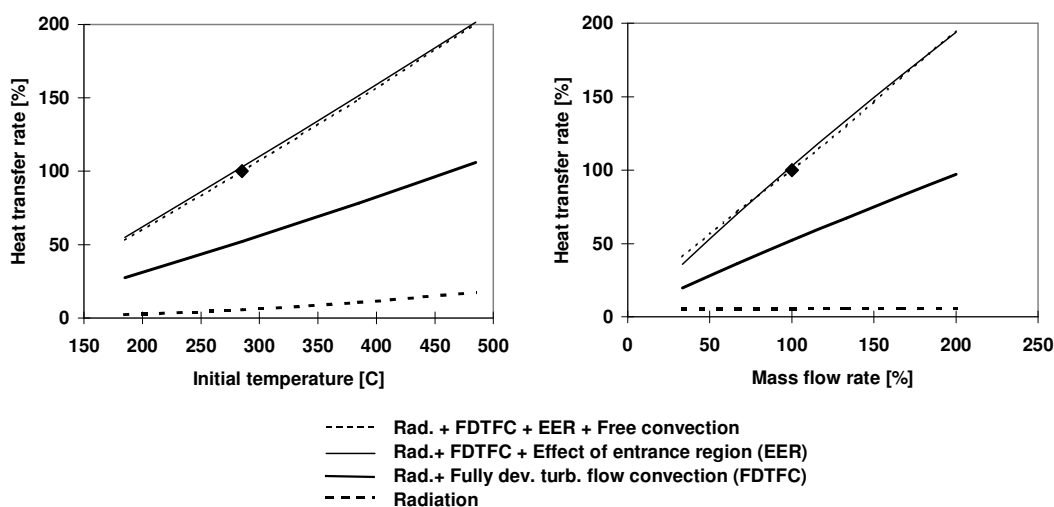


Figure 18. Change in heat transfer rate of the convection section with varying initial temperature and the mass flow rate of flue gas. Full load case is shown with a black symbol.

The correction factor of the Nusselt number is independent of the mass flow rate and of the flue gas temperature. Thus, the relative effect of the entrance region on the heat transfer should be constant. However, this is not true in either of the cases as is shown in Fig. 18. This is because the heat transfer rate includes the effect of radiation. On the left, the portion of the radiation of the whole heat transfer rate increases, and the effect of the convection and thereby that of the entrance region decreases, when changing the flue gas initial temperature from 185 to 485 °C.

Radiation also has an effect in the case of changing mass flow rate, on the right. When the mass flow rate increases, the radiative heat transfer increases concurrently with the mean temperature of the flue gas. However, the increase of the convective heat transfer is stronger, and the relative portion of the radiation decreases significantly when increasing the mass flow rate from one third to double value of the full load. The effect of entrance region increases.

The effect of natural convection is small and mostly reducing the heat transfer, but at minimum mass flow its portion is approximately 14 % of the total heat transfer rate.

The next four analyses depict the designer's possibilities to exploit the simulation method for optimising the construction.

When using straight and smooth tubes, the designer is able to change three geometrical parameters of a tube: number n , length l , and diameter d . In Figures 19 and 20 the parameters vary but the initial data is the same as in Tab 1, Exp.1 in Paper VI.

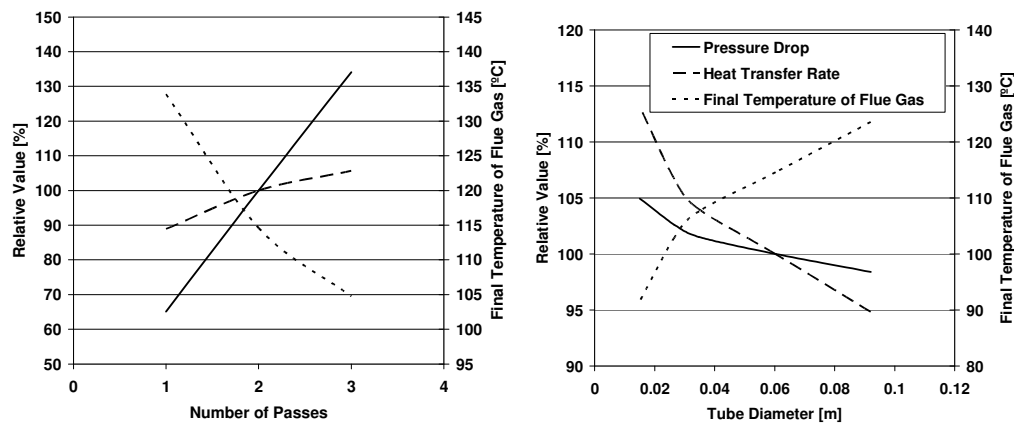


Figure 19. Effect of dividing the convection section into 1, 2 or 3 passes (on the left) and effect of using different tube diameters (on the right). To the right, total cross-section area and inner heat transfer surface area of tubes remain constant (Paper VI).

The convection section of the pellet boiler has two passes. The effect of dividing it into one or three passes is shown in Fig. 19 on the left (n , d and total l are constant). The tube diameter and the heat transfer area are constant. It means that with one pass the tube length is double and with three passes it is $2/3$ compared to the reference case. With three passes the heat transfer rate increases by 6 %, and with one pass it decreases by 11 %. The final flue gas temperature decreases by 10°C and increases 19 °C, respectively. This is caused by the effect of the entrance region. However, the gradient of the heat transfer rate decreases when the number of passes increases whilst Fig. 16 would suggest an increase in gradient. The reason for this is that concurrently with the decreasing difference in temperature between flue gas and water the heat transfer rate also decreases.

The pressure drop becomes double when adding the number of passes from 1 to 3. Hence, the inlet and the outlet of the tubes dominate the pressure drop. The pressure drop due to friction for the entire tube length is equal to the pressure drop of the inlet and outlet of one pass.

The outer diameter of the pellet boiler tube is 60.3 mm. Tube diameter is changed using one larger and three smaller ones (see Fig. 19 on the right). The inner heat transfer area and the cross sectional flow area are constant (i.e., also n and l of the tubes change). When decreasing the diameter the initial bulk flow velocity stays constant, but the Reynolds number decreases and the friction factor slightly increases. It also follows that the value of Nu decreases but not proportionally to the diameter. Therefore, the relative heat transfer rate increases more than the pressure drop. It means that, using a smaller diameter; the heat transfer area can be exploited in a more efficient way. Modern bio-fuel boilers have an impeller for combustion air or flue gas so that natural draft is not the only force driving the flow. In principle, the selection of tube diameter is a question of economic optimisation.

In Figure 20 the heat transfer area is changed using two different methods. On the left, the number of tubes n varies (d and l are constant), and on the right, d and n vary keeping the total cross-flow section area of the tubes constant (i.e. l and initial v are constant).

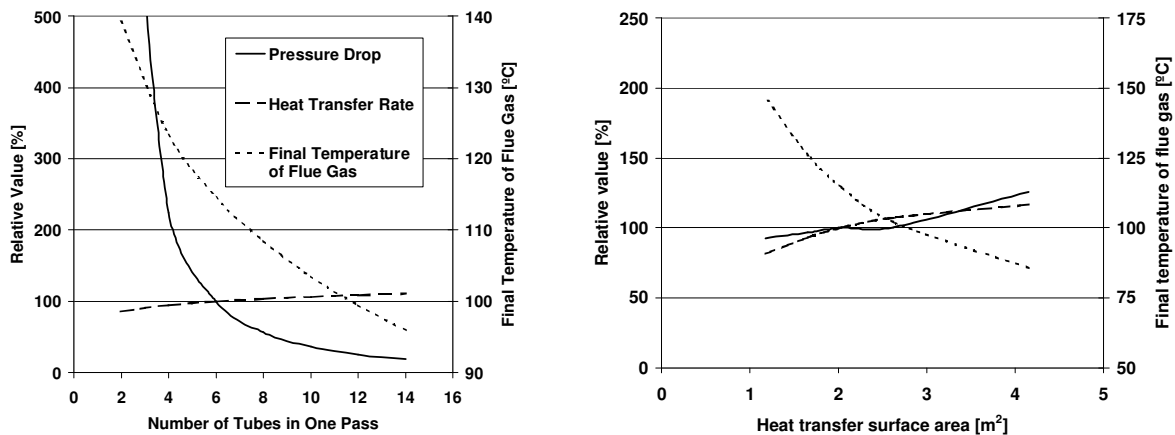


Figure 20. The effect of decreasing or increasing the number of convection tubes from the original value $n = 6$ (on the left) and decreasing or increasing the heat transfer area from the original value (on the right) (Paper VI).

The heat transfer rate decreases by 15 % when the number of tubes decreases from the original 6 to 2, and the rate increases by 9 % when the number of tubes increases from 6 to 14, see Fig. 20 on the left. The gain with 8 additional tubes is smaller than the loss with 4 tubes less. The inner heat transfer coefficient decreases due to the decrease in flue gas velocity when the number of tubes is increased. Secondly, the mean temperature difference between flue gas and boiler water decreases which decreases the heat transfer rate. On the other hand, the pressure drop increases by 800 % and decreases by 75 %, respectively.

When the heat transfer area is increased, keeping the total cross-flow section area of tubes constant the heat transfer rate increases more than in the previous case, see Fig. 20, on the right. The increase is 16 % when the heat transfer is doubled from the original value $A = 2.03 \text{ m}^2$. This is because the changes of the inner heat transfer coefficient are smaller due to the constant initial velocity of the flue gas. Unlike the previous case, the pressure drop changes in the opposite

direction because the friction factor increases with decreasing tube diameters. However, the range of the pressure drop is smaller, from 92 to 125 % when the heat transfer increases from 56 to 200 %.

4.2 Rectangular convection section with fins

4.2.1 Modelling

The initial data for modelling are the geometry of the finned surface and the mass flow rate, the initial temperature and composition of flue gas, and the temperature of the boiler-water, see Fig. 21.

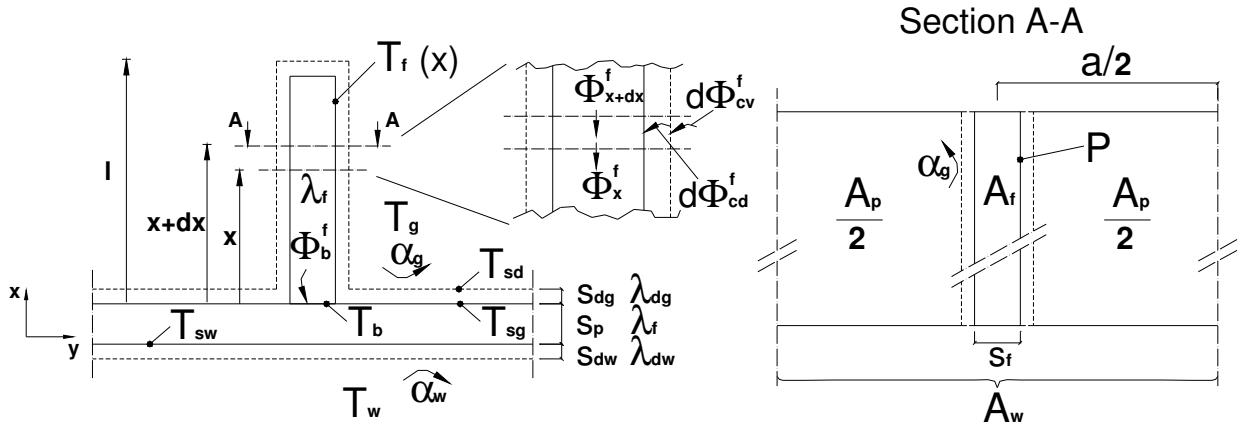


Figure 21. Schema of the model of a fin element (Paper V).

Heat transfer in a single fin can be derived from stationary heat balances in Eqs. (9) and (10), on the assumption that heat conduction in the fouling layer is negligible in the direction parallel to the fin (x-direction).

$$\phi_x^f = \phi_{x+dx}^f + d\phi_{cd}^f \quad (9)$$

$$d\phi_{cd}^f = d\phi_{cv}^f = (P + 4s_{dg})dx(T_g - T_f) / (1/\alpha_g + s_{dg}/\lambda_{dg}) \quad (10)$$

A change in the heat transfer rate inside the fin can be calculated with Eq. (11), on the assumption that the thermal conductivities and cross sections of the fin and the fouling layer are constant, and further that the temperature gradient is positive and conduction is a diminishing function in the x-direction.

$$\frac{d\phi_x^f}{dx} = -\lambda_f A_f \frac{d^2 T_f}{dx^2} \quad (11)$$

By using notations

$$m^2 = (P + 4s_{dg}) / \left[\lambda_f A_f \left(1/\alpha_g + s_{dg} / \lambda_{dg} \right) \right] \quad (12)$$

and

$$\theta = T_g - T_f \quad (13)$$

the differential equation describing the temperature change along the fin becomes

$$\frac{d^2\theta}{dx^2} - m^2\theta = 0. \quad (14)$$

Assuming a constant heat transfer coefficient from the tip to the base of the fin the boundary condition at the tip is

$$-\lambda_f \frac{d\theta}{dx} \Big|_{x=l} = \theta \Big|_{x=l} / \left(1/\alpha_g + s_{dg} / \lambda_{dg} \right) \quad (15)$$

The base temperature is assumed to be known

$$\theta \Big|_{x=0} = \theta_b = T_g - T_b \quad (16)$$

The rate of heat transfer of the fin can be solved

$$\phi_b^f = \lambda_f m A_f \frac{\sinh ml + (p/m) \cosh ml}{\cosh ml + (p/m) \sinh ml} (T_g - T_b). \quad (17)$$

where

$$p = 1 / \left[\lambda_f \left(1/\alpha_g + s_{dg} / \lambda_{dg} \right) \right] \quad (18)$$

Assuming that both the thickness of the fouling layer and the heat transfer coefficient are constant for the entire element (plate + fin) and that the heat conductivity of the element is infinite in the direction of the plate (y -direction), the base temperature of the fin is equal to the surface temperature of the plate ($T_{sg} = T_b$), and the heat transfer rate to the plate is

$$\phi^p = A_p (T_g - T_b) / \left(1/\alpha_g + s_{dg} / \lambda_{dg} \right). \quad (19)$$

It also follows that the surface temperature of the waterside T_{sw} is uniform and, hence, heat transfer of the entire element is

$$\phi_b^f + \phi^p = (A_f + A_p)(T_b - T_w) / \left(1/\alpha_w + s_{dw} / \lambda_{dw} + s_p / \lambda_f \right). \quad (20)$$

An opposite assumption is that the thermal conductivity of the plate is zero in the y-direction. In that case the heat transfer of the fin and that of the plate must be calculated separately. The actual solution is somewhere between these two ultimate assumptions, because the heat conductivity in the homogenous material is equal in the x and y directions ($\lambda_{f,y} = \lambda_{f,x}$). The results calculated according to these two assumptions were compared with the results from the commercial ANSYS-program, which uses a numerical two-dimensional finite element method [42]. The comparison is shown in Fig. 22.

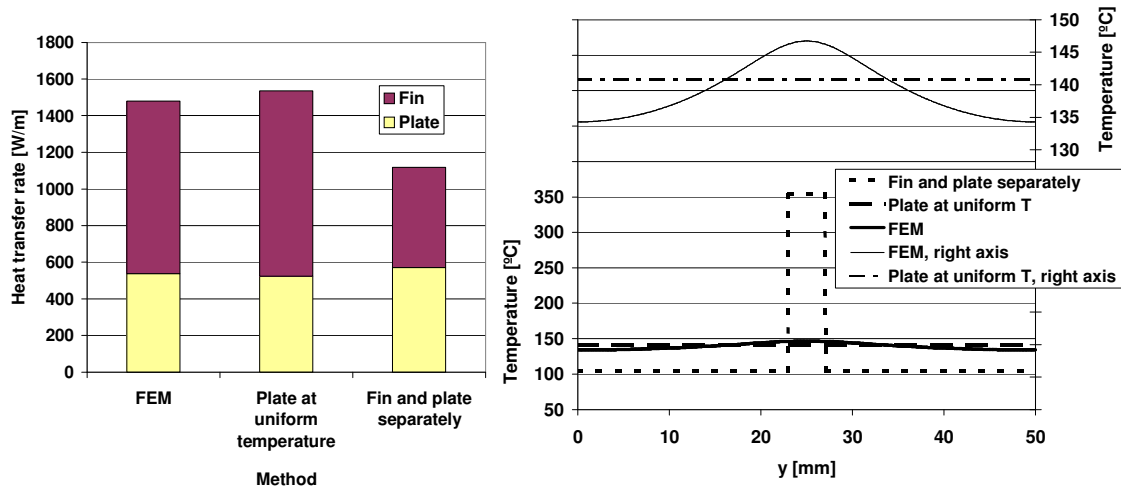


Figure 22. A comparison of the heat transfer rate (on the left) and the corresponding surface temperatures T_{sw} (on the right) between three methods (Paper V).

Initial data in Fig 4.7 is: $\alpha_g = 25 \text{ Wm}^{-2}\text{K}^{-1}$, $\alpha_w = 500 \text{ Wm}^{-2}\text{K}^{-1}$, $T_g = 600 \text{ }^\circ\text{C}$, $T_w = 80^\circ\text{C}$, $\lambda_f = 52 \text{ Wm}^{-1}\text{K}^{-1}$, $l = 50 \text{ mm}$, $a = 50 \text{ mm}$ ($y = 0 \rightarrow 50 \text{ mm}$), $s_f = 4 \text{ mm}$, $s_p = 6 \text{ mm}$, $s_{dg} = s_{dw} = 0 \text{ mm}$.

On the assumption that $\lambda_{f,y} = \infty$ (plate at uniform temperature) the heat transfer rate is closer to the result of the FEM calculation than when assuming that $\lambda_{f,y} = 0$ (fin and plate separately), see the bars on the left. The latter gives the smallest rate of heat transfer, especially for the fin. On the assumption that $\lambda_{f,y} = 0$, the surface temperature T_{sw} rises unrealistically high at the fin, see the right graph. This decreases the heat transfer rate of the fin. Elsewhere the temperature T_{sw} is lower than with other methods. Further, on the assumption that $\lambda_{f,y} = \infty$, the temperature T_{sw} is constant and between the extreme values of the FEM calculation, which is shown in detail on the right axis. The case of a fouled fin is shown in Fig. 23.

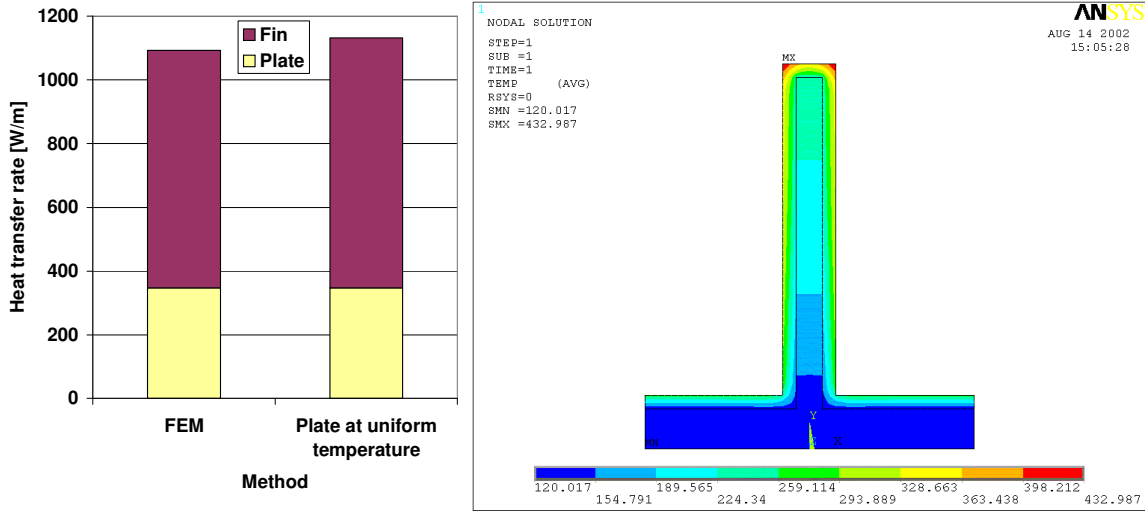


Figure 23. A comparison of the heat transfer rate of a fouled fin between FEM and the simplified method (on the left) and the corresponding temperature field using the FEM calculation (on the right), where temperatures are in °C (Paper V).

The data for fouling in Fig. 23 is $s_{dg} = 2$ mm, $s_{dw} = 0$ mm, $\lambda_{dg} = 0.12$ WK⁻¹m⁻¹, other initial data is similar to the data in Fig. 22.

The simplified method with a fouled fin gives a 3.6 % higher heat transfer rate than the FEM calculation. The difference was 3.7 % with the clean fin in Fig. 22. The case of a fouled fin in Fig. 23 is similar to the case of a clean fin in Fig. 22 as far as fluid flows and geometry are concerned. Thus, in this example the fouling layer reduces the heat transfer rate by 24.7 %.

4.2.2 Analyses

In the model the pass of the convection section can be divided into an optional number of computational cells in the direction of the flue gas flow. The calculation algorithm is based on the simultaneous numerical solving of the enthalpy change and the total heat transfer rate of the finned plate elements and end walls.

$$-\dot{m}_{fg} \frac{\partial h}{\partial z} = n(\phi_b^f + \phi^p) + \phi^{ep} \quad (21)$$

The heat transfer rate of the end walls is calculated analogically with the plate. The heat transfer coefficient of the waterside is assumed constant. The heat transfer coefficient of the flue gas side is calculated by the method described in Section 4.1.1 by replacing the diameter with a hydraulic diameter of $d_h = 4A_{cs}/U$. The heat transfer coefficient is assumed to be constant in the entire cell, and the temperature of the ambient flue gas is assumed uniform at the whole cross-section (= at the plate and along the height of the fin).

In Fig. 24 a sensitivity study of the heat transfer rate of the element (plate + fin) is shown when the values of some key parameters are changed one by one from one fourth to the fourfold of the assumed typical value.

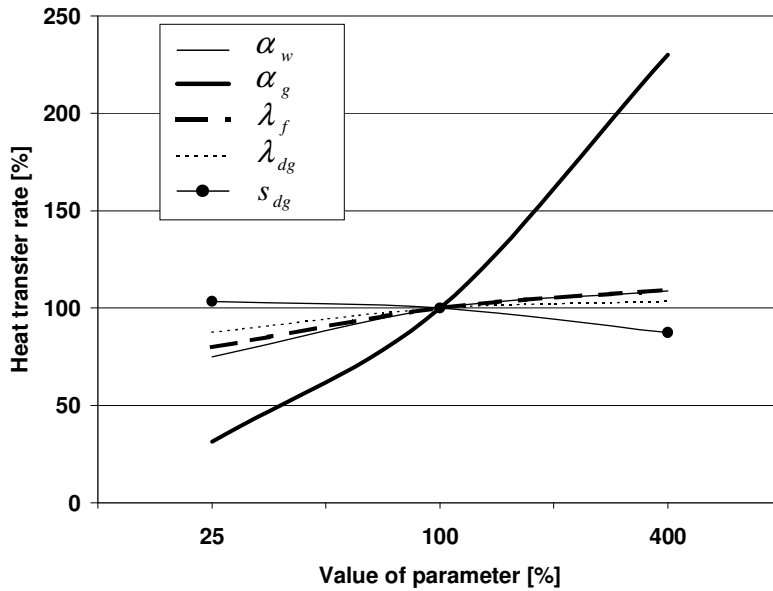


Figure 24. The effect of some parameters on the heat transfer rate of an element (plate+fin) (Paper V).

The assumed typical values at point 100 % in Fig. 24 are $\alpha_g = 25 \text{ Wm}^{-2}\text{K}^{-1}$, $\alpha_w = 500 \text{ Wm}^{-2}\text{K}^{-1}$, $\lambda_f = 52 \text{ Wm}^{-1}\text{K}^{-1}$, $\lambda_{dg} = 0.1 \text{ Wm}^{-1}\text{K}^{-1}$, $s_{dg} = 0.25 \text{ mm}$, $s_{dw} = 0 \text{ mm}$.

The heat transfer coefficient of the gas side has the strongest influence on the heat transfer rate, and the thermal conductivities have the weakest influence.

However, the thickness of the fouling layer grows in the course of time, increasing the fuel consumption. Typically, the operation staff can only observe the flue gas exhaust temperature. With the simulation it is possible to calculate the relationship between the flue gas temperature, loss in the heat transfer rate and thickness of the deposit, see Fig. 25. This helps estimate the appropriate cleaning periods, taking into account the fuel consumption and the cleaning costs.

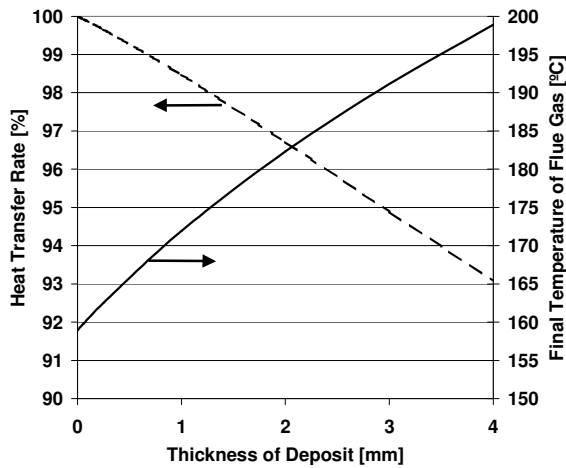


Figure 25. The relative heat transfer rate of the convection section and the final temperature of flue gas as a function of thickness of the deposit (Paper V).

4.3 Discussion

Convection section with tubes

A significant difference between the measured and calculated heat transfer rates of the wood pellet boiler was found. The most probable cause for this is assumed to be the inaccuracy in the correlation of the entrance region. Firstly, the full-scale equipment differs from the experimental apparatus used in the laboratory setting. When compared to those in the literature, the clearest difference is in the configuration of the entrance region. Secondly, the accuracy was good in the wood chip boiler in which the effect of the entrance region is insignificant ($z = 60.1$). An adequate accuracy was also achieved on air-flue gas heat exchangers with long tubes ($z = 81$) in Paper III. Further still, Neshumayev *et al.* have found a similar feature during the measurement of one 200 kW_{th} oil-fired boiler and a 20 kW_{th} wood pellet boiler. The experimental convective heat transfer was higher than that obtained using the calculation data. Neshumayev *et al.* explain the difference by the presence of strong entrance effect (Neshumayev *et al.* 2003). Thus, correcting the calculation addresses the constants C and m in Eqs. (6)...(9). Unfortunately, the experimental program was not extensive enough to come to a definite conclusion. CFD modelling could have given more information on the thermal performance of the entrance region, but it was not possible to do within this study. The fluctuation of the flue gas flow is considered as one possible reason for the difference in the Paper VI. It has been suggested that the unsteadiness of the flow could increase the heat transfer [53, 54], but also controversial results have achieved [55]. The oscillation of the flow is not measured in this study, and therefore the possible effect of it is not studied further.

The model offers optimization possibilities to the designer. There are, however, practical limitations on the construction. First, the demand for thermal efficiency and the risk of local condensation of water vapour set an upper and lower limit for the flue gas temperature,

respectively. Secondly, the convection section must have a self-cleanable feature, which sets a minimum flue gas velocity and an upper limit for the diameter. Sweeping is difficult on small diameter tubes which sets a lower limit for the diameter. Thirdly, manufacturing technology, transportation, and installation delimit the shape and size alternatives. After selecting valid alternatives, it is possible to calculate their thermal performance and pressure drop. In addition to this, decision-making requires taking manufacturing and material costs into account. The model is also suitable for water boilers using different fuels with no limitation on the size of the boiler. It also offers a sizing strategy, but additional validation measurements are needed if the dimensionless tube length is short and the shape of the convection section differs from the tested one.

The portion of radiation is 3 - 13 % of the whole heat transfer rate at typical biomass boiler conditions. The portion of the effect of entrance region is 39 - 52 % in the pellet boiler and the effect of natural convection is small mostly reducing the heat transfer, but at a minimum load it reached up to +14 %.

Dividing the convection section into more passes causes the heat transfer rate to increase, even if the heat transfer surface area is constant. This is because the effect of the entrance region multiplies.

The heat transfer area is exploited in a more efficient way by using smaller tube diameters, even if the bulk velocity of the flow remains constant. The increase in the heat transfer surface area by increasing the number of tubes increases the heat transfer rate only slightly. This feature is in accordance with the well-known Reynolds analogy [19, 20]. By reducing the diameter concurrently with an increased number of tubes, it is possible to keep the cross-flow area constant and achieve a greater improvement to the heat transfer rate.

Rectangular convection section with fins

The model of a finned convection section includes several simplifying assumptions. Firstly, some of them have a minor influence on the result. The thermal conductivity of the plate-fin element is assumed to be infinite in the y-direction. This leads to uniform base and plate temperature. The FEM calculation leads from 2 to 6 % lower values of the heat transfer rate in a wide range of initial data. Hence, by multiplying the result by a constant factor of 0.96, the accuracy is always at least ± 2 % compared with the FEM calculation. Thermal conductivity of an element is an input value in the program. It is known for the applied material and the influence of changes from one quarter to the fourfold of a default value of $52 \text{ WK}^{-1}\text{m}^{-1}$ is -20 to 9 % in the heat transfer rate, respectively, see Fig. 24. The conductivity is assumed to be independent of temperature, which is a usual idealizing assumption [27, 28, 43]. According to [1] the difference of the conductivity is 10 - 15 % between at the tip temperature and at the base temperature. The convective heat transfer coefficient of the waterside is assumed to be constant; it is also an input value in the simulation program. The impact of changing it from a default value of $\alpha_w = 500 \text{ Wm}^{-2}\text{K}^{-1}$ to 125 and $2000 \text{ Wm}^{-2}\text{K}^{-1}$ is -25 and 9 % in the heat transfer rate, respectively. The first value is unrealistically low for heat transfer from hot surface to water, a range of $300 \dots 600 \text{ Wm}^{-2}\text{K}^{-1}$ is reported to be appropriate for free convection [4]. In that case, changes in the heat transfer rate

are -10 and 3 %, respectively. Thus, the changes anticipated in the waterside heat transfer coefficient have only a small effect on the heat transfer rate.

Secondly, the assumptions and the initial data concerning fouling are both uncertain and may have a significant effect on the result, see Figs. 22, 23 and 24. Fouling is modelled in Ch. 4.2.1 by its thickness and thermal conductivity. The effect of fouling is often known only for its effect on the total heat transfer rate. In such a case, fouling is described as a heat transfer resistance (= fouling factor R). However, in an illustrative simulation program, it would be easier for the user to perceive the mean thickness than the heat resistance value of fouling. Hesselgreaves prefers the use of conductivity and thickness for practical reasons. In this approach, it is possible to take simultaneously into account the demands for acceptable decrease in heat transfer and increase in pressure drop [44]. The thermal conductivity of boiler scale components is greater than that of the ash on the flue gas side, though a wide range of variety is given both for ash and actual boiler scale [20, 21, 45, 46, 47]. The assumptions of constant thickness of a fouling layer and its negligible heat conductivity in the direction parallel to the fin, Eq. (11), are theoretical. The former may cause a significant error but the latter probably not, because it is for 1 - 3 orders of magnitude lower than the conductivity of the fin.

Thirdly, it was found difficult to estimate the heat transfer coefficient of the flue gas side having the most significant effect on the results. Radiation of the radiating gas components CO_2 and H_2O has been included in the model, but radiation between the fin and the plate is excluded. The effect of gas radiation was found to be 3 - 10 % of the total heat transfer, because the temperature and concentration of radiating components are relatively low and the effective thickness of the gas layer is small. Convective heat transfer coefficient is assumed to be constant along the height of the fin. Mokheimer has found a marked improvement on the fin efficiency under natural convection by using a variable heat transfer coefficient [48]. Naik et al. have measured threefold to fourfold values of the local Nu number at the tip of the fin compared to the base of it in turbulent forced convection, if there is a clearance above the fin [49]. However, the distance between adjacent fins in our convection section is large, 3.75-fold compared to that of the test arrangement in [50] and the change is probably smaller. There is minimum fin spacing in the convection section to allow cleaning. The deposit is typically mechanically removed and the array of fins must not make it difficult. The fin spacing is more than double compared to the optimal value calculated by the empirical correlation proposed in [49].

The convective heat transfer coefficient changes in the direction of the flow because of the developing flow conditions and the changes in properties of gas. Kalman and Laor state that the local heat transfer coefficient of a longitudinal fin depends on the location along the flow path in the turbulent forced convection [27]. Naik et al. describe a significant improvement in the heat transfer coefficient in the middle of the long rectangular fin compared to its end [49].

Verification measurements for the model of a finned convection section were conducted at the laboratory of VTT Processes in Jyväskylä on an Arimax BIO 300 boiler. Results were also compared with the field measurements on an Arimax BIO 500 boiler at Pori Forest institute in Kullaa and with the measurements on an Arimax BIO 1000 boiler at the Sports Institute of Finland in Vierumäki [50]. The boiler used at VTT was new, and the convection sections of the boilers in Kullaa and Vierumäki had been cleaned just before measurements. According to the

measurements the model seems to describe the effects of changes in the operating conditions with reasonable accuracy. However, additional measurements are needed for convection sections of different shapes or sizes to ensure an accurate result for a certain operating stage.

Using the model it is possible to study the performance of different convection sections equipped with rectangular longitudinal fins of constant thickness, and it can be used as a tool for dimensioning and development work. It also helps the operation staff to estimate an appropriate cleaning period.

5 HEAT EXCHANGER

5.1 Flue gas heat exchanger

5.1.1 Modelling

The flue gas heat exchanger (FGHEX) used in the boiler plant is shown in Fig. 6. The primary flow of FGHEX is hot flue gas and the secondary flow is outside air which is preheated by the exhaust gas heat exchanger. The heat exchanger is of a pipe-bundle type where flue gas flows in pipes and outside air on the shell side. The cross-flow elements are arranged in a counter-flow configuration, see Fig. 26.

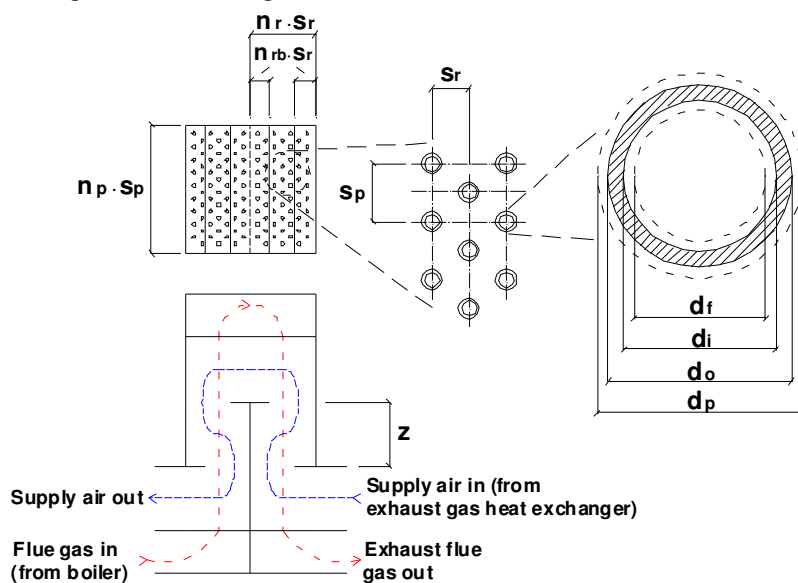


Figure 26. The principle construction of the FGHEXs in the pilot and demonstration plant (Paper III).

The principle of modelling is similar to the modelling of the convection part. The calculation of heat transfer coefficients is described in Paper III. Some simplifying assumptions are made. The isolated heat exchanger is assumed to be fully tight and adiabatic, thus the leakage flow and heat transfer from or to the environment are excluded. Also the leakage between primary and secondary flows is excluded, but in the shell the leakage stream through the gap around the tubes and by-pass stream through the gap between the baffle and the shell are taken into account. Also, the effect of radiation is excluded because the diameter of the tubes and the partial pressure of carbon dioxide and water vapour are small and the temperature of the flue gas is relatively low. Finally, in calculating the convective heat transfer coefficient the effects of the entrance region of turbulent flow and mixed convection are omitted, because the tubes are relatively long compared to their diameter and the natural convection is assumed to be insignificant.

5.1.2 Analyses

Fig 27 shows comparison calculations with changed mass flow rates and heat transfer surface areas. The proportional heat output changes rather linearly according to changes in mass flows. The heat transfer rate is low when the type of flow changes from turbulent to laminar. No sudden decrease in the heat transfer rate appears.

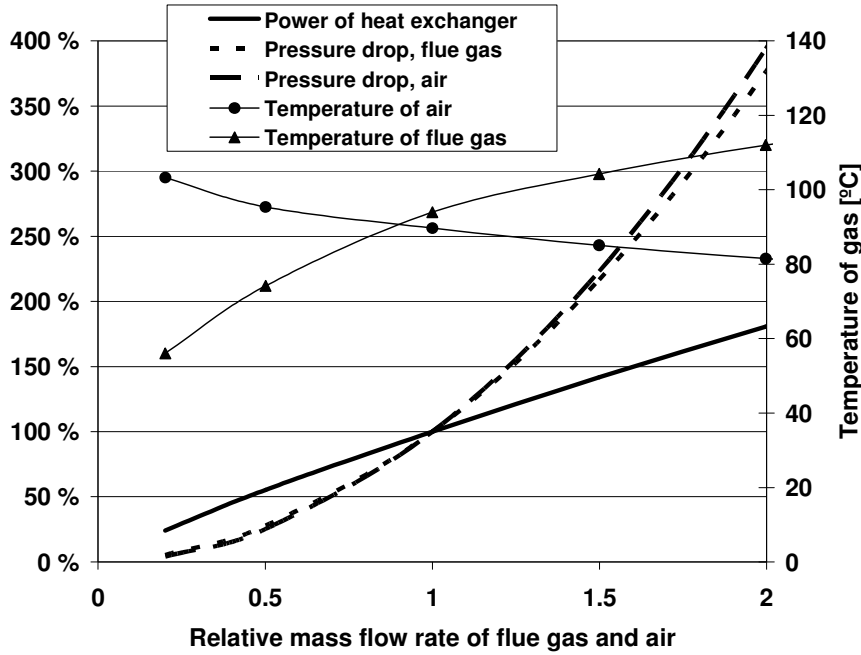


Figure 27. Heat effect, pressure drops and outlet temperatures as a function of the rate of mass flow of air and combustion gas (changed in the same proportion) (Paper I).

In Fig. 28 the comparison of four different flow arrangements is shown. Changing the arrangement of flows influences the characteristics of the heat exchanger. Input data of calculation is shown in Table 2. The boiler plant is operating at a peak load of 500 kW. The molar composition of inlet flue gas is $\text{CO}_2(\text{H}_2\text{O})_{1.81}(\text{N}_2)_{7.81}(\text{O}_2)_{1.05}\text{Ar}_{0.08}$.

Table 2. Input data of the FGHEX calculations.

Data of flows		
Flue gas mass flow rate, kg/s		0.576
Air mass flow rate, kg/s		2.227
Geometry and material properties		
	1. Section	2. Section
Tube outer diameter, d_o , mm	42.4	42.4
Tube wall thickness, $(d_o - d_i)/2$, mm	2.6	1.5
Fouling layer thickness, $(d_i - d_f)/2$, mm	0.5	0.5
Distance betw. adjacent pipes in the row, s_p , mm	60	60
Distance between adjacent rows, s_r , mm	80	80
Number of pipe rows, n_r	10	8
Number of pipe rows in a baffled zone, n_{rb}	5	4
Number of pipes in one row, n_p	11	11
Distance between baffles, z *, m	1	1
Diameter of perforation in the baffle, d_p , mm	44	44
Gap between the baffle and shell, mm	2	2
* z in heat exchanger type d , m	1.5	1.5
Heat conductivity of the tube material, $W K^{-1} m^{-1}$	52	25
Heat conductivity of the fouling, $W K^{-1} m^{-1}$	0.12	0.12

The heat exchangers have the same heat transfer area and tube geometry. The only exception is heat exchanger type **d** which has only one baffle resulting in a larger cross-sectional area for the secondary flow and thus a smaller velocity of air. The symbols describing the geometry of the FGHEX are shown in Fig. 26.

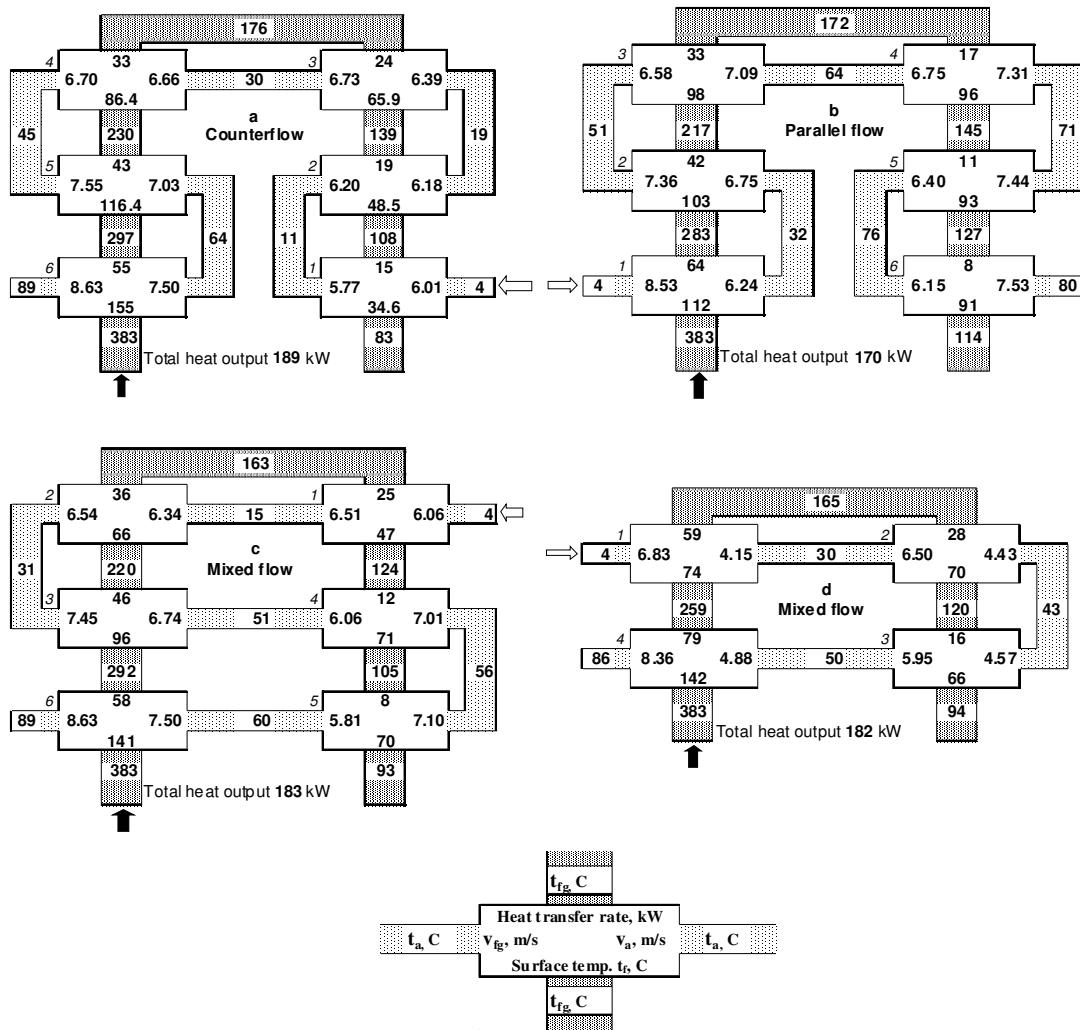


Figure 28. Comparison of four types of heat exchangers: **a)** counter-flow, **b)** parallel-flow, **c)** mixed-flow with two baffles, **d)** mixed-flow with one baffle (Paper III).

A counter-flow type heat exchanger gives the highest outlet temperature of air. This is beneficial, because after the heat exchanger, the air is led to combustion and drying. If combustion air temperature increases, the propagation velocity of the ignition front in the fuel bed and the heat effect of the boiler increase. If the drying air temperature increases, the needed mass flow rate decreases. On the other hand, it is not desirable that the surface temperature of the inside wall of the tubes falls below the dew point of water vapour in the flue gas. The dew point of the flue gas is 56 °C, which on type **a** is broken up in cells 1 (34.6 °C) and 2 (48.5 °C) and on type **c** in cell 1 (47 °C), respectively.

5.2 Drying exhaust gas heat exchanger

5.2.1 Modelling

The primary flow of the drying exhaust gas heat exchanger (DEGHEX) is moist exhaust gas from the drying silo. Its temperature range is about 20 - 40 °C and it is nearly saturated. The secondary flow is outside air, see Fig. 6. A flat-plate type was chosen due to low investment costs, see Fig. 29.

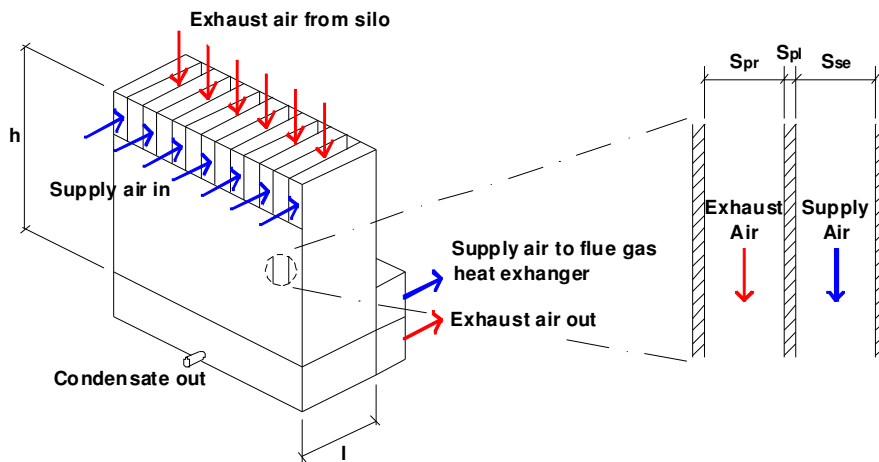


Figure 29. The principle construction of the DEGHEX in the demonstration plant (Paper III).

The principle of modelling is similar to that of the convection part. An additional matter is the effect of condensation. The calculation of condensation and heat transfer coefficients is described in Paper III. Some simplifying assumptions are made. Firstly, the heat resistance of the fouling is excluded. Secondly, the isolated heat exchanger is assumed to be fully tight and adiabatic, and the leakage flow and heat transfer from or to the exterior are excluded. Also, the leakage between primary and secondary flows is excluded. Thirdly, the heat resistance of the condensate layer is excluded and the outlet condensate temperature is assumed to be equal to that of the outlet gas.

5.2.2 Analyses

The comparison of different flow arrangements is shown in Fig. 30. The heat exchanger is divided into 3 computational cells on the parallel-flow and counter-flow types, and into 9 cells on the cross-flow type. The mass and heat balances of the cells are calculated by means of the heat balance of a single plate [1, 5, and 51]. The procedure of the calculation is similar to that in the case of the flue gas heat exchanger. The surface temperatures and air temperatures leaving the different types of heat exchangers are shown in Fig. 30. The pressure drop of the heat exchanger is calculated according to [1].

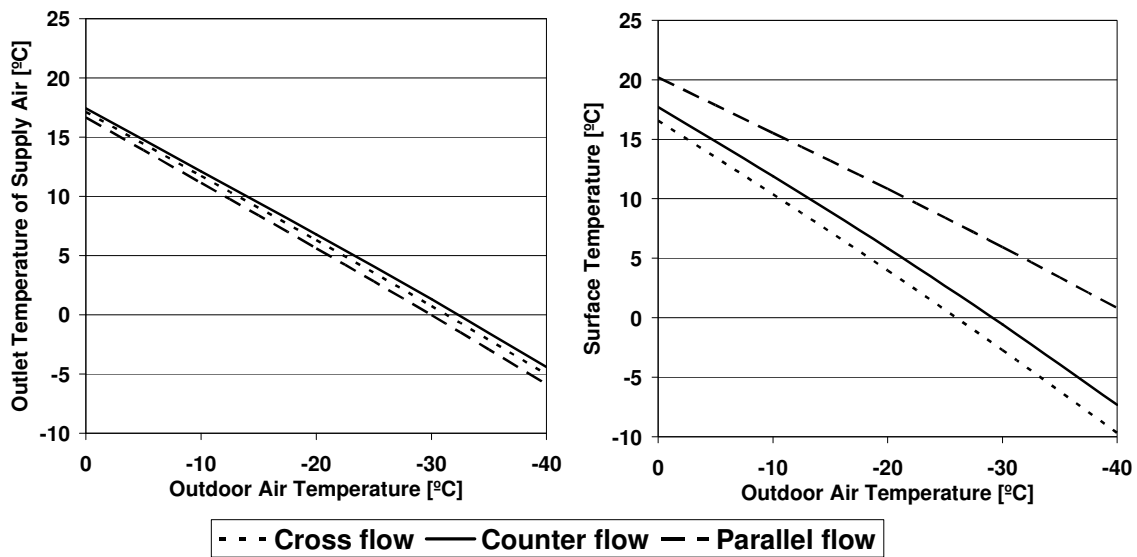


Figure 30. Outlet temperature and surface temperature in different types of heat exchangers (Paper I).

Temperatures of the outlet supply air are shown on the left-hand side and the lowest surface temperatures (in the middle of the computational cell) on the right-hand side depending on the entering outdoor air temperature and the type of the heat exchanger. The rates of mass flow, heat transfer area and the properties of the entering moist exhaust air of the drying silo are constant.

The outlet air temperatures are rather close to each other on different types of heat exchangers. The temperature difference between the counter-flow and parallel-flow is 1 °C, when the outdoor air temperature is 0 °C and 2 °C when -40 °C, thus the heat outputs are also almost equal. The outlet temperature of the cross-flow heat exchanger is between these types. The surface temperatures differ more. In regard to freezing, a critical outdoor temperature appears when the lowest surface temperature falls below 0 °C. Freezing appears at an outdoor air temperature of -26 °C on a cross flow, -28 °C on a counter flow and below -40 °C on a parallel flow heat exchanger at the critical rates of mass flows. In countries of temperate climate the counter-flow heat exchanger is more beneficial than other types because the heat transfer rate is greater, see Fig. 30.

The effect of DEGHEX in the system is illustrated in Fig 31. The DEGHEX reduces the FGHEX's heat output demand, which is needed to raise the drying air temperature to a sufficient level. Furthermore, it improves the efficiency of the boiler plant by recovering some heat of the exhaust gas to drying and combustion air. In that sense, this boiler plant operates in a similar way as do the boiler plants with a flue gas condensing system; the exhaust gas heat exchanger condenses a part of the water evaporated from the fuel particles. The input data of a case where the moisture content of fuel is 45 % (wb) as received is shown in Table 3.

Table 3. Input data of calculations. The symbols describing the geometry of the heat exchanger are shown in Fig. 29.

	Primary	Secondary				
Distance between plates, s_{pr}, s_{se} , mm	15	10				
Number of passes, n_{pr}, n_{se}	15	16				
Thickness of the plate, s_{pl} , mm		2				
Conductivity of the plate material, $W K^{-1}m^{-1}$		52				
Depth of the plates, I , m		1				
Height of the plates, h , m		4				
	Outside temperature t_1 , °C					
	-30	-20	-10	0	10	20
Heat output of the plant, kW	500	500	500	500	293	125
Heat output of the flue gas heat exch., kW	101	99	96	90	49	7
RH%, outside air	80	80	80	80	80	70
RH%, drying exhaust gas	86	87	88	89	93	32

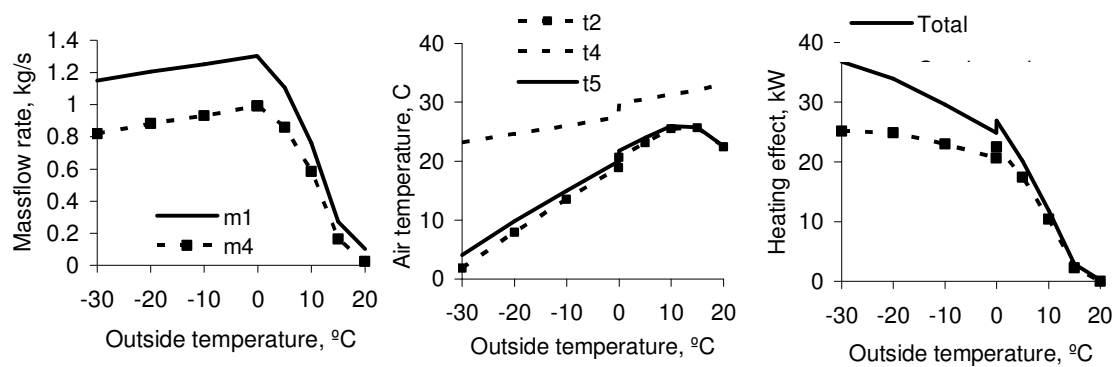


Figure 31. Mass flow rates, temperatures and the heat transfer rate of the DEGHEX. The notes of mass flows and temperatures refer to Fig. 6 (Paper III).

In Fig. 31 the mass flow rates and inlet temperature are results of the heat and mass balance calculations of the system. The mass flow rates decrease slightly when the outdoor temperature is below 0 °C, because with a decreasing outdoor temperature, the damper, TV01, starts to shut slowly. The temperatures of both flue gas (t_7) and combustion/drying air (t_3) are kept constant at 110 and 90 °C by the control system, respectively. While the outdoor temperature decreases, the heat demand of the FGHEX increases. The mass flow rate of the combustion air is independent of the outdoor temperature. Thus, the only adjustable variable is the mass flow rate of the drying air. The damper, TV01 reduces both the primary and secondary mass flow rates of the DEGHEX. The heat load of the boiler plant reduces when the outdoors temperature exceeds 0 °C, see Table 3, therefore also the mass flow rates decrease distinctively. The smaller the mass flow rate of the fuel is, the smaller are the mass flow rates of all the gases.

By enlarging the plate area of the parallel-flow heat exchanger, practically no additional heat is transferred. In the centre of Fig. 31 is shown that the difference of the outlet temperatures varies

from 0.01 ($t_1 = 20 \text{ }^\circ\text{C}$) to 2.3 $^\circ\text{C}$ ($t_1 = -30 \text{ }^\circ\text{C}$). On the other hand, the minimum outlet temperature of the primary flow is 4 $^\circ\text{C}$ ($t_1 = -30 \text{ }^\circ\text{C}$) and there is a risk of freezing when changing the flow arrangement into cross-flow or counter-flow. Furthermore, Fig. 30 establishes that no significant increase in heat output is achieved with a cross-flow or a counter-flow type heat exchanger. This is because of the large share of condensation in the total heat output of the exhaust gas heat exchanger (68 - 88 % in Fig. 31, on the right).

When the outside temperature exceeds 0 $^\circ\text{C}$, there is a jump in the primary inlet temperature (t_4). In this stationary modelling, it is assumed that at frost the fuel is icy and at 0 $^\circ\text{C}$ it immediately melts. Because the drying air temperature is kept constant and no heat is needed for melting any more, the temperature of the exhaust drying air increases by 2.3 $^\circ\text{C}$ in this example. Naturally there also appears to be a temperature step in the outlet mass flows (t_2, t_5), too.

For reliability reasons, moving parts have not been applied to protect against freezing. The heat output of the exhaust gas heat exchanger increases with increasing the heat load of the plant. In that sense, the exhaust gas heat exchanger has self-regulation characteristics. On the basis of Paper III, it can be concluded that without the exhaust gas heat exchanger the outlet temperature of the flue gas will decrease below the dew point. On the other hand, when designing the system so that the outlet temperature of the flue gas always remains above the dew point, the outlet combustion gas temperature from the boiler should exceed 500 $^\circ\text{C}$ in the dimensioning condition. This is considered to be difficult to realise without expensive solutions in the boiler designing. Consequently, a practical alternative for the exhaust gas heat exchanger may be the storage of dry fuel for the duration of extreme cold weather. The exhaust gas heat exchanger decreases the yearly fuel consumption. With the initial values shown in the Table 3 and Fig. 31, the calculation gives an estimate of 4.5 % for the yearly fuel consumption.

5.3 Discussion

One 40 kW_{th} pilot plant was built purely for experimental purposes, and one 500 kW_{th} demonstration plant both for experimental purposes and producing heat to the users during the development work.

One FGHEX was tested at the pilot plant and one at the demonstration plant. Both of them are of a counter-flow type which was considered as the best type at the beginning of the study. This choice caused condensation of flue gas at low outside temperatures and always during the start-up of the plant. The partial load situations also lead to condensation, because no control (by-pass or recirculation) of the flows is installed in those plants. It was observed that fly ash particles stuck on the inner wet surface of the tubes causing fouling which finally resulted in a plug preventing the flow in the condensing area. The condensate and particles formed a sticky solution in the cells 1 and 2 where the tube surface was wet, see Fig. 28. After drying, the deposit was difficult to remove. The thin easily removable layer of grey pulverized fly ash was discovered in the tubes in cells 4, 5 and 6.

Two DEGHEXs were tested at the demonstration plant. The first was a small-scale device mainly for verifying the modelling and observing the operational characteristics and the second was a full-scale device for minimizing the condensation problem of the FGHEX.

The dust leaving the drying silo causes fouling on the surfaces of the heat exchanger. To minimize dust emissions a dust collector was installed between the dryer and the heat exchanger.

Because of the pressure loss of the primary flow, the drying air must be maintained over - pressurised before the drying silo. The drying silo is open to the ambient air at the top and to the screw feeder at the bottom. The over-pressure caused leakage of the moist air to the conveyor channel and the fuel storage. This led to freezing problems in the fuel storage at frost. An extra exhaust gas fan was installed after the heat exchanger.

The operational aspects of the whole system limit the possibilities to optimise the heat effect and dimensions of the heat exchangers. The maximum inlet temperature to the heat exchanger from the boiler type considered is approximately 400 °C. If it increases, more expensive materials will be needed in the combustion chamber and the probability of slag forming increases. The softening temperature of wood ash is 1100 - 1200 °C [52], but slagging may form at temperatures clearly below this. Thus, adding the masonry of the walls of the combustion chamber increases the risk of local slagging on the grate. The minimum exhaust flue gas temperature from the FGHEX derives from the dew point of flue gas, being in the range of 70 - 100 °C depending among other things on the moisture content of fuel, and on the construction of the heat exchanger. The temperature of the drying air must be clearly below 250 °C which is the ignition temperature of wood. The control strategy must ensure that the temperature does not even accidentally exceed the chosen safety level. Due to emissions a maximum temperature of 100 °C is recommended [17]. On the other hand, increasing the drying air temperature improves the efficiency of the boiler plant. The maximum inlet air temperature depends on the dimensioning of the exhaust drying gas heat exchanger. The dimensioning outdoor temperature in Finland is - 26...-38 °C depending on the region of the country. The inlet temperature to the heat exchanger is in the range of 20 - 35 °C and it is almost saturated. Consequently, the freezing risk limits the minimum exhaust air temperature.

Calculating the combinations of extreme operating conditions (heat load, moisture content of fuel, outside temperature) gives the input data needed for comparing different types of heat exchangers, dimensioning the heat transfer area, choosing the control strategy and selecting operating parameters and set-values of the control system. Using well-known engineering correlations for heat and mass transfer, an adequate degree of accuracy between the model and validating measurements was achieved.

6. CONCLUSIONS

Efforts to restrict the emissions of greenhouse gases will increase the use of forest bio fuels. A large range of moisture content is one of the most significant difficulties in combustion of wood chips in the grate boiler plants. One possibility to manage the problem of varying moisture content is to dry fuel with warm air at the boiler plant. This shortens and simplifies the fuel chain but requires additional equipment to be supplied to the boiler plant. This thesis introduces two alternative boiler plants with a convective warm air dryer. The first one dries wood chips for the use of the plant itself. Outdoor air is heated in two stages, *i.e.*, preheated with heat recovered from the exhaust drying air and heated with heat recovered from the flue gas. In addition to the dryer, the second alternative is also equipped with a sieve to produce fuel to the market. Outdoor air is heated by a heat exchanger connected in parallel with the heating network. This kind of a boiler plant has notable direct and indirect benefits. It gives farmers or other members of the energy co-operative a possibility to earn extra income. The load of the boiler plant is more stable than that in the traditional district heating use. Therefore, controlling of the combustion improves and also problems of a minimum load use are avoidable. Indirect advantages are, among others, savings in investments because the boilers can be designed smaller and simpler for small-scale users due to the high quality of fuel. The grate area, heat transfer area and volume of the combustion chamber decrease. The homogenous fuel enhances possibilities for an accurate control of combustion, which improves efficiency and reduces pollutant combustion emissions from small-scale boilers. The idea to use the reserve heating effect for drying is the principal technical novelty of this study.

There are thermal interdependencies between the boiler, dryer and heat exchangers, and in addition the ranges of heating load, moisture content of fuel and outdoor air temperature are large. These features make the design of the boiler plant with a dryer complex. Therefore, the objective of the study has been to develop models so as to better understand and predict the thermal performance of the system in changing operational conditions. Six models are described, two for each equipment under study, the dryer, the convection section and the heat exchanger.

A simplified energy and mass balance model as well as a deep bed model were developed for the dryer. The energy and mass balance model was used for analysing the energy consumption, size and fan power of the dryer. The deep bed model is based on the shrinking core single-particle model. The single-particle model is implemented in the model of the deep bed. With this model the profiles of MC inside the bed were calculated. The MC may increase from the initial value at the back end of the bed where the water vapour condenses on the surface of the fuel particles. Models for the dryer have been verified by measurements in the laboratory test rig in Satakunta University of Applied Sciences. The calculated rate of evaporation compares well with the measurements but the air temperature inside the bed differs more. Long-term practical operation results were collected in a 40 kW_{th} pilot plant and in a 500 kW_{th} demonstration plant.

Drying of a fixed bed of material is clearly a two-stage process for a deep bed, if the short initial heat-up period is not considered. In the first stage, the air outlet temperature is constant as shown by the measurements and also predicted by the model. Then air at the outlet is practically saturated and the mass release of water from the fixed bed is constant and the average moisture decreases. In the second stage, the outlet temperature starts to increase and the humidity to

decrease. The rate of drying decreases, and finally, the equilibrium moisture is reached, if the drying time is long enough. Case analyses of the energy and mass balance show that specific energy consumption for drying does not significantly depend on the drying air temperature. In wintertime the specific energy consumption is slightly smaller with high drying air temperature than with low temperature, but in summertime the situation is reverse.

A model was developed to calculate the heat transfer rate and pressure loss of the convection section with tubes and another one for the convection section with a rectangular duct having an array of longitudinal rectangular fins for flue gas. Contrary to expectations, the model for the convection section with tubes underestimated the heat transfer rate of the convection section of the 50 kW_{th} pellet boiler approximately by 40 %. This is more than could be expected due to the reported inaccuracy in the correlations for heat transfer in the literature. The accuracy with the wood chip boiler was adequate. The effect of the entrance region was estimated as the most uncertain part in the calculations, because it has notably a greater influence on the heat transfer rate of the short tubes in the pellet boiler than on that of the long tubes in the wood chip boiler. A method was proposed where the corrections are focused on the constants of the correlation of the entrance region. After correction the model also predicted performance in the varying operating conditions of the pellet boiler with a good degree of accuracy.

Case analyses showed that the portion of radiation of the whole heat transfer rate is small in typical biomass boiler conditions. The portion of effect of the entrance region is 39 - 52 % in the pellet boiler and the effect of natural convection is small mostly reducing the heat transfer. Secondly, dividing the convection section into more passes causes the heat transfer rate to increase, even if the heat transfer surface area is constant. This is because the effect of the entrance region is multiplied. Thirdly, the heat transfer area is exploited in a more efficient way by using smaller tube diameters, even if the bulk velocity of the flow remains constant. Further, an increase in the heat transfer surface area by adding the number of tubes increases the heat transfer rate only slightly. By reducing the diameter concurrently by increasing the number of tubes, the cross-flow area can be kept constant and a greater improvement to the heat transfer rate is achieved.

Heat transfer was modelled for the finned surface with a fouling layer. In a few details, this modification differs from the equations derived for the clean finned surface. The assumption of uniform base temperature was compared to the results from the finite element method. This assumption is practicable in modelling. The heat transfer coefficient from flue gas to surface showed clearly to be the most influential parameter affecting the heat transfer rate of the convection section.

The model for the convection section with tubes was verified by laboratory measurements of the 50 kW_{th} pellet boiler in the laboratory of the manufacturer and by field measurements of 4000 kW_{th} wood chip boiler. The model for the finned convection section has been verified by laboratory measurements of the 300 kW_{th} wood chip boiler in the laboratory of VTT and by field measurements of 500 and 1000 kW_{th} wood chip boilers.

Two heat exchangers are described and modelled, a pipe-bundle type flue gas heat exchanger and a flat plate type drying exhaust gas heat exchanger. As a result of the case analyses, a counter-

flow type flue gas heat exchanger was found inapplicable to the boiler plant with a dryer. This is because condensation of water vapour is unavoidable in the dimensioning conditions for this type. Condensation makes the fouling sticky. On the other hand, the heat output is insufficient with a parallel-flow type. Therefore, a mixed-flow type was found most appropriate. There, cross-flow elements are arranged partly for counter-flow and partly for parallel-flow. A parallel-flow type was found most appropriate as the drying exhaust gas heat exchanger because of the smallest risk of freezing and nearly equivalent heat output with other types. The heat outputs differ only slightly due to the big share of the condensation heat. The drying exhaust gas heat exchanger decreases the required heat from the flue gas to the drying air by preheating the drying air. This characteristic is indispensable in order to minimize condensation in the flue gas heat exchanger. It also saves fuel by recovering heat from the exhaust drying air back to the system. Its yearly fuel savings in the district heating example were estimated to be 4.5 %.

Fouling was detected as a major problem with the FGHEX. However, in the absence of condensation, the increase in the fouling layer with respect to time was observed low. Fouling was a problem also with the DEGHEX, but the condensation of moisture in the exhaust drying air was not found to have an adverse effect on cleaning. After the installation of a simple dust collector a reasonable cleaning period was achieved.

The model for the tube-bundle type flue gas heat exchanger was verified by measurements on the 40 kW_{th} pilot plant and 500 kW_{th} demonstration plants. The model for the flat-plate type exhaust drying air heat exchanger was verified by measurements on the 500 kW_{th} demonstration plant. A reasonable accuracy for the models was achieved.

Mathematical modelling proved to be a useful means to develop a heating plant for moist and dry bio fuel. Modelling of thermal behaviour of the plant helps in understanding interdependencies of the two heat exchangers, the boiler and the dryer.

In this study, a concept by which wood chips of good quality (moisture, particle size) can be produced for small-scale heating systems in connection with district heating has been developed. The wood fuel of low quality is used in the plant itself. District heating plants using wood operate much under their maximum effect most of the year during which the excess heat output can be used for drying. In this way, the need and costs to build a separate heat producer for the dryer is avoided. The production of marketable wood chips has also several beneficial effects on the heat production of the plant itself, for example, during the summer season. In addition to this concept the sub-systems (dryer, heat exchangers) have been discussed and studied by modelling for technical optimization.

The production of marketable fuel in connection with district heating will promote the commercial use of biomass in two ways. Firstly, the extra income from sellable fuel will improve the economy of the heat entrepreneur. Secondly, good quality wood fuel improves the operation and control of small-scale heating systems, which can lead to cheaper furnaces with lower emissions.


REFERENCES

- [1] VDI-Gesellschaft Verfahrenstechnik und Chemieingenieurwesen (Hrsg.). VDI-Wärmeatlas, Berechnungsblätter für den Wärmeübergang, 9. Auflage. Springer-Verlag, Berlin, 2000. (in German)
- [2] Huhtinen M, *et al.* Höyrykattilatekniikka. 5. Ed., Oy Edita Ab, Helsinki 2000. (in Finnish)
- [3] Raiko R, *et al.* Poltto ja palaminen, 2. Ed., 2002 (in Finnish)
- [4] Wagner W. Wärmeübertragung, 2. überarbeitete Aufl. Vogel, Würzburg, 1988 (in German).
- [5] Hewitt G F (Ed.). Heat Exchanger Design Handbook. Begell House Inc., New York, 1998.
- [6] Hakkila P. Review of the wood energy technology programme in 1999 - 2003, in: Final Report of the Wood Energy Technology Programme in 1999 - 2003. VTT, Jyväskylä, 2004, pp. 11 - 19
- [7] Anttila, V., Market analysis of drying of wood chips and sawdust (in Finnish), Bs. Thesis, Satakunta Polytechnic, Pori, Finland, 2002
- [8] Rupar-Gadd K. A parameter study of drying and storage of biomass, Växjö University, Licentiate Thesis, 2003.
- [9] Nurmi J. Characteristics of whole-tree biomass for energy, PhD Thesis, University of Helsinki, The Finnish Forest Research Institute, Research Papers 758, 42 p., 2000.
- [10] Lundgren J, Hermansson R, Dahl J. Experimental studies of a biomass boiler suitable for small district heating systems. Biomass and Bioenergy 2004;26:443 - 54.
- [11] Rupar K, Sanati M. The release of terpenes during storage of biomass. Biomass and Bioenergy 2005;28:29 - 34
- [12] Krischer, O.; Kast, W. Die Wissenschaftlichen Grundlagen der Trocknungstechnik. Springer-Verlag; Berlin/Heidelberg, 1978, 489 p.
- [13] Key R. B. Introduction to Industrial Drying Operations, Pergamon Press, Great Britain, 1978.
- [14] Johansson I, Larsson S, Wennberg O. Torkning av biobränslen med spillvärme. Värmeforsk Service AB, report A4 - 312, 74 p., 2004. (in Swedish).

- [15] Wahlund B, Yan J, Westermark M. A total energy system of fuel upgrading by drying biomass feedstock for cogeneration: a case study of Skellefteå bioenergy combine. *Biomass and Bioenergy* 2002;23:271 - 81
- [16] Ståhl M, Granström K, Berghel J, Renström R. Industrial processes for biomass drying and their effects on the quality properties of wood pellets. *Biomass and Bioenergy* 2004;27:621 - 29
- [17] Holmberg H, Ahtila P. Comparison of drying costs between multi-stage drying and single-stage drying. *Biomass and Bioenergy* 2004;26:515 – 30
- [18] Fagnäs L, Sipilä K. Emissions of biomass drying. Proceedings of the Conference on Developments in Thermochemical Biomass Conversion, Banff, Canada, 20 - 24 May, 1996.
- [19] Incropera FP, Dewitt DP. Fundamentals of heat and mass transfer, 4th ed. Wiley, New York, 1996.
- [20] Mills AF. Heat and mass transfer. Richard D Irwin Inc., U.S., 1995.
- [21] Isachenko VP, Osipova VA, Sukomel AS. Heat transfer. Mir Publishers, Moscow, 1977.
- [22] Aung W, Kakac S, Shah RK (Eds.). Handbook of single-phase convective heat transfer. Wiley, New York, 1987.
- [23] Aicher T, Martin H. New correlations for mixed turbulent natural and forced convection heat transfer in vertical tubes. *Int. J. Heat Mass Transfer* 1997;40 (15):3617 - 26.
- [24] Hausen H. Darstellung des Wärmeüberganges in Rohren durch verallgemeinerte Potenzbeziehungen. *Z. Ver. Dtsch. Ing., Beiheft Verfahrenstech.* 1943;4:91 - 134.
- [25] Grass G. Wärmeübertragung an turbulent strömende Gase im Rohreinlauf. *Allg. Wärmetechnik* 1956;7(3).
- [26] Neshumayev D, Ots A, Laid J, Tiikma T. 2003. Heat Transfer Augmentation and Pressure Drop of Turbulator Inserts in Gas-heated Channels. In *Advances in Heat Transfer Engineering*, 4th Baltic Heat Transfer Conference, Kaunas, Lithuania, Sundén B, Vilemas J. Eds., Begell House; 565-572
- [27] Laor K, Kalman H. Performance and optimum dimensions of different cooling fins with a temperature-dependent heat transfer coefficient. *Int. J. Heat Mass Transfer* 1996;39 (9):1993 - 2003.
- [28] Razelos P, Kakatsios X. Optimum dimensions of convecting-radiating fins: Part I – longitudinal fins. *Applied Thermal Engineering* 2000;20:1161 - 92.

- [29] Wiksten R. Fins of Heat Exchangers, in: Lampinen M (Ed.). Dimensioning of heat exchangers. Helsinki University of Technology, Laboratory of Applied Thermodynamics, Otaniemi, 1997 (in Finnish).
- [30] Isdale JD, Mercier P, Grillot JM, Mulholland A, Gomatam J. Integrated modelling of process heat transfer with combustion and fouling. *Applied Thermal Engineering* 1997;17 (8 - 10):751 - 62
- [31] Saastamoinen J, Impola R. Drying of biomass particles in fixed and moving beds. *Drying Technology* 1997;15 (6 - 8):1919 - 29.
- [32] Good J, Neuenschwander P, Nussbaumer Th. Grundlagen der Abgaskondensation bei Holzfeuerungen. Ingenieurbüro Verenum. 80 p., Zürich 1998 (in German)
- [33] Good J, Neuenschwander P, Nussbaumer Th. Combustion efficiency in biomass furnaces with flue gas condensation. Biomass for energy and industry, 10th European Conference and Technology Exhibition. Würzburg, Germany 1998.
- [34] Saastamoinen JJ, Kilpinen PT, Norström TN. New simplified rate equation for gas-phase oxidation of CO at combustion. *Energy & Fuels* 2000;14 (6):1156 - 60.
- [35] Saastamoinen JJ, Taipale R. NO_x formation in grate combustion of wood, *Clean Air, International Journal on Energy for a Clean Environment* 2003;4 (3):30 p.
- [36] Staiger B, Unterberger S, Berger R, Hein KRG. Development of an air staging technology to reduce NO_x emissions in grate fired boilers. *Energy* 2005;30:1429 - 38.
- [37] Thunman H, Leckner B. Ignition and propagation of a reaction front in cross-current bed combustion of wet biofuels. *Fuel* 2001;80:473 - 81.
- [38] Koistinen R. Fundamentals of fuel bed combustion in grate firing (in Finnish). VTT Research Notes 622, 102 p., Espoo 1989.
- [39] Honkasalo M, Yrjölä J. Kattilalaitostekniikka kuiville ja kosteille biopolttoaineille. In: Bioenergian tutkimusohjelma vuosikirja 1997 osa III, pp. 169 - 79. Jyväskylä (in Finnish).
- [40] Malling GF, Thodos G. Analogy between mass and heat transfer in beds of spheres: Contributions due to end effects. *Int. J. Heat Mass Transfer* 1967;10: 489 - 98.
- [41] Huff ER. Effect of size, shape, density, moisture and furnace wall temperature on burning times of wood pieces. *Fundamentals of Thermochemical Biomass Conversion*, Estes Park, USA, 1982; Overend RP, Milne A, Mudge LK. Eds.; Elsevier Applied Science Publishers, New York: Great Yarmouth, Great Britain, 1985: 761 - 75.
- [42] ANSYS Program Online Guide Release 3.55

- [43] Yeh R-H. An analytical study of the optimum dimensions of rectangular fins and cylindrical pin fins. *Int. J. Heat Mass Transfer* 1997;40 (15):3607 - 15
- [44] Hesselgreaves JE. An approach to fouling allowances in the design of compact heat exchangers. *Applied Thermal Engineering* 2002;22:755 - 62.
- [45] Bott TR, *Fouling of Heat Exchangers*, Elsevier, Amsterdam 1995
- [46] Chenoweth JM, General design of heat exchangers for fouling conditions, in: Melo LF et al. (Eds.), *Fouling Science and Technology*, Kluwer Academic Publishers, Dordrecht, Netherlands, 1988.
- [47] Taborek J. Assesment of fouling research on the design of heat exchangers, in: Panchal CB (Ed.), *Fouling Mitigation of Industrial Heat Exchange Equipment*, Begell House Inc., New York, 1997.
- [48] Mokheimer EMA. Heat transfer from extended surfaces subject to variable heat transfer coefficient. *Heat and Mass Transfer*, 2002;39(2):131 - 38
- [49] Naik S, Probert SD, Bryden IG. Heat transfer characteristics of shrouded longitudinal ribs in turbulent forced convection. *Heat and Fluid Flow* 1999;20:374 - 84.
- [50] Huttunen M, Kjälman L, Paavilainen J, Saastamoinen J, Yrjölä J. Modelling of a Grate Boiler. CODE Technology Programme for Modelling of Combustion Processes, Technical Review 1992-2002. TEKES, Helsinki, 2003: 129-38.
- [51] Lampinen M. Mass transfer, Helsinki University of Technology. Laboratory of Applied Thermodynamics, Otaniemi, 1997 (in Finnish).
- [52] Wilen C, Moilanen A, Kurkela E. 1996. Biomass feedstock analyses. Technical Research Centre of Finland, VTT Publications 282, Espoo.
- [53] Hanby V. Convective heat transfer in a gas fired pulsating combustor. *Journal of Engineering for Power (ASME)* 1969;91:48 - 52.
- [54] Sridhar Thyageswaran. Numerical modelling of pulse combustor tail pipe heat transfer. *International Journal of Heat and Mass Transfer* 2004;47:2637 - 2651
- [55] Barker AR, Williams JEF. Transient measurements of the heat transfer coefficient in unsteady, turbulent pipe flow. *International Journal of Heat and Mass Transfer* 2000;43:3197 - 3207



ISBN-13 978-951-22-8438-2
ISBN-10 951-22-8438-3
ISBN-13 978-951-22-8439-9 (PDF)
ISBN-10 951-22-8439-1 (PDF)
ISSN 1795-2239
ISSN 1795-4584 (PDF)